

Guidelines

Thai Guideline for Nuclear Medicine Investigations of Neurocognitive Disorders: Nuclear Medicine Society of Thailand, the Neurological Society of Thailand, and Thai Medical Physicist Society Collaboration

Tawika Kaewchur ^{1,2}, Tanyaluck Thientunyakit ³, Wichana Chamroonrat ⁴, Benjapa Khiewvan ³,
Peerapon Kiatkittikul ⁵, Nantaporn Wongsurawat ⁶, Chanisa Chotipanich ⁵, Yuttachai Likitjaroen ⁷,
Vorapun Senanarong ⁸, Panya Pasawang ⁹, Tanawat Sontrapornpol ⁹, Nucharee Poon-iad ³,
Sasithorn Amnuaywattakorn ⁴ and Supatporn Tepmongkol ^{10,11,12,13,*}

- ¹ Division of Nuclear Medicine, Department of Radiology, Faculty of Medicine, Chiang Mai University, Chiang Mai 50200, Thailand; tawika.k@cmu.ac.th
- ² PET/CT and Cyclotron Center, Center for Medicine Excellence, Faculty of Medicine, Chiang Mai University, Chiang Mai 50200, Thailand
- ³ Division of Nuclear Medicine, Department of Radiology, Faculty of Medicine Siriraj Hospital, Mahidol University, Bangkok 10700, Thailand; stanyalu@hotmail.com (T.T.); benjapa.khi@mahidol.ac.th (B.K.); fortune_nucharee_si@hotmail.com (N.P.-i.)
- ⁴ Division of Nuclear Medicine, Department of Diagnostic and Therapeutic Radiology, Faculty of Medicine Ramathibodi Hospital, Mahidol University, Bangkok 10400, Thailand; wichana.cha@mahidol.edu (W.C.); amsasithorn@gmail.com (S.A.)
- ⁵ National Cyclotron and PET Centre, Chulabhorn Hospital, Chulabhorn Royal Academy, Bangkok 10210, Thailand; peerapon.kia@cra.ac.th (P.K.); chanisa.ja@gmail.com (C.C.)
- ⁶ Division of Nuclear Medicine, Department of Radiology, Faculty of Medicine, Khon Kaen University, Khon Kaen 40002, Thailand; nantwo@kku.ac.th
- ⁷ Department of Medicine, Faculty of Medicine, Chulalongkorn University and King Chulalongkorn Memorial Hospital, Thai Red Cross Society, Bangkok 10330, Thailand; yuttachai.l@chula.ac.th
- ⁸ Department of Internal Medicine, Faculty of Medicine, Siriraj Hospital, Mahidol University, Bangkok 10700, Thailand; vorasenanarong@yahoo.com
- ⁹ Division of Nuclear Medicine, Department of Radiology, King Chulalongkorn Memorial Hospital, Bangkok 10330, Thailand; ppasawang@gmail.com (P.P.); santi_s@hotmail.com (T.S.)
- ¹⁰ Division of Nuclear Medicine, Department of Radiology, Faculty of Medicine, Chulalongkorn University, Bangkok 10330, Thailand
- ¹¹ Chulalongkorn University Biomedical Imaging Group (CUBIG), Faculty of Medicine, Chulalongkorn University, Bangkok 10330, Thailand
- ¹² Chula Neuroscience Center, King Chulalongkorn Memorial Hospital, Thai Red Cross Society, Bangkok 10330, Thailand
- ¹³ Center of Excellence in Cognitive Impairment and Dementia, Faculty of Medicine, Chulalongkorn University, Bangkok 10330, Thailand
- * Correspondence: supatporn.t@chula.ac.th



Citation: Kaewchur, T.; Thientunyakit, T.; Chamroonrat, W.; Khiewvan, B.; Kiatkittikul, P.; Wongsurawat, N.; Chotipanich, C.; Likitjaroen, Y.; Senanarong, V.; Pasawang, P.; et al. Thai Guideline for Nuclear Medicine Investigations of Neurocognitive Disorders: Nuclear Medicine Society of Thailand, the Neurological Society of Thailand, and Thai Medical Physicist Society Collaboration.

Diagnostics **2024**, *14*, 2474. <https://doi.org/10.3390/diagnostics14222474>

Academic Editor: Andreas Kjaer

Received: 10 October 2024

Revised: 28 October 2024

Accepted: 29 October 2024

Published: 6 November 2024



Copyright: © 2024 by the authors. Licensee MDPI, Basel, Switzerland. This article is an open access article distributed under the terms and conditions of the Creative Commons Attribution (CC BY) license (<https://creativecommons.org/licenses/by/4.0/>).

Abstract: Nuclear medicine investigations play a significant role in diagnosing dementia, mainly using imaging techniques such as positron emission tomography (PET) and single-photon emission computed tomography (SPECT). By providing functional and molecular data via brain imaging, nuclear medicine investigations offer valuable insights that complement clinical evaluations and structural imaging in the early detection, diagnosis, and differentiation of various types of dementia, leading to more accurate diagnosis and personalized treatment planning. Therefore, the Nuclear Medicine Society of Thailand, the Neurological Society of Thailand, and the Thai Medical Physicist Society have collaborated to establish these practical nuclear medicine investigation guidelines aiming to (1) identify the role of nuclear medicine studies in patients with neurocognitive disorders; (2) assist referrers in requesting the most appropriate procedure for diagnosis of each type of neurocognitive disorders; and (3) identify scientific evidence that is useful to assisting nuclear medicine professionals in recommending, performing, interpreting, and reporting the results of nuclear medicine investigations in patients with neurocognitive disorders.

Keywords: positron emission tomography (PET); single-photon emission computed tomography (SPECT); dementia; neurocognitive disorders; guidance

1. Introduction

Dementia is a syndrome of cognitive decline in different domains. Regarding the etiologies, neurodegenerative brain disease is the most common cause of dementia in the elderly, followed by cerebrovascular diseases. The clinical diagnosis of neurodegenerative brain disease causing dementia is based on clinical criteria [1]. Various neurodegenerative diseases causing dementia have been defined by their clinical syndromes and neuropathological findings, such as Alzheimer's disease, dementia with Lewy bodies, frontotemporal lobar degeneration, and their variants. The definite diagnosis of neurodegenerative brain disease needs the findings of pathological protein accumulation and neuronal degeneration within the brain parenchyma. Each disease has a specific pattern of brain atrophy and type of accumulated protein, which is revealed during an autopsy [2–4]. Nonetheless, obtaining brain tissue for diagnosis is impractical due to its invasiveness.

Previously, brain imaging in dementia, including computed tomography (CT) and magnetic resonance imaging (MRI), was used to rule out reversible causes of dementia, such as cerebrovascular disease, hydrocephalus, tumors, etc. Although modern high-resolution MRI can precisely demarcate gray matter, white matter, and other non-brain parenchymal structures, leading to the detection of gray and white matter change patterns in individuals with neurodegenerative brain disease, molecular imaging such as single-photon emission computed tomography (SPECT) and positron emission tomography (PET) further allow indirect observation of the pattern of functional brain decline or pathological protein accumulation, which are more specific to the disease. The overlaps among clinical syndromes, pathological protein accumulation, and genetic risk are the challenges of dementia diagnosis. Thus, various imaging techniques have been added to diagnostic criteria to improve dementia care in clinical and dementia research [5–8].

Since the number of dementia patients in Thailand is increasing along with the aging society, there are rising demands for dementia investigations. (In Thailand, accessibility to MRI, SPECT, and PET is still limited, and the cost of these imaging studies is high. Therefore, it is necessary to have guidelines for choosing the most appropriate diagnostic techniques for an individual patient). These guidelines aim to assist clinicians and nuclear medicine specialists in diagnosing, choosing appropriate nuclear medicine investigations, performing image acquisition, interpreting images, and being aware of potential pitfalls in using SPECT and PET in neurocognitive disorders.

2. Definitions

Dementia is a syndrome of insidious cognitive decline in one or more domains that is significant from the previous level of cognition. The decline must be severe enough to interfere with occupational, social, or daily life functions. According to the fifth version of the Diagnostic and Statistical Manual of Mental Disorders version 5 (DSM5), revised by the American Psychiatric Association (APA) in 2013 [9], the term major neurocognitive disorder is used as an alternative name for dementia. Mild cognitive impairment (MCI) is also a syndrome of cognitive decline with less severity that does not interfere with occupational, social, or daily life functions. MCI was introduced in order to define the pre-symptomatic dementia [10]. Mild neurocognitive disorder is an alternative term for MCI according to DSM5.

Moreover, MCI has been declared as a disease. In addition, the cognitive domains have been revised and renamed as complex attention, executive function, learning and memory, language, perceptual-motor, and social cognition [9,11]. The causes of dementia can result from various diseases. Each type of dementia has a specific clinical syndrome, diagnostic criteria, brain pathologic findings, and structural and functional change patterns. This

information must be assessed before choosing the appropriate investigations. These guidelines discuss the main roles of molecular imaging (SPECT and PET) in assisting in clinical diagnosis and management of neurocognitive disorders associated with neurodegenerative diseases (Table 1).

Table 1. Common types of dementia related to neurodegenerative diseases.

| | |
|-----------------------------------|---|
| Alzheimer’s disease (AD) | |
| Alzheimer’s disease (AD) variants | Posterior cortical atrophy (PCA) Logopenic aphasia (PCA) Frontal variant AD (fvAD) Corticobasal syndrome (CBS) variant AD Familial AD |
| Non AD dementia | Lewy body dementia (LBD) <ul style="list-style-type: none"> - Dementia with Lewy bodies (DLB) - Parkinson’s disease dementia (PDD) Frontotemporal lobar degeneration (FTLD) <ul style="list-style-type: none"> - Behavioral variant FTLD (bvFTLD) - Primary progressive non-fluent aphasia (PNFA) - Semantic dementia (SD) Vascular dementia (VaD) |

3. Objectives

1. To identify the role of nuclear medicine studies in patients with neurocognitive disorders.
2. To assist referrers in requesting the most appropriate procedure for the diagnosis of each type of neurocognitive disorder.
3. To identify scientific evidence that is useful in assisting nuclear medicine professionals in recommending, performing, interpreting, and reporting the results of nuclear medicine investigations in patients with neurocognitive disorders.

4. Guideline Development and Recommended Flow of Nuclear Medicine Investigations of Dementia Syndrome

The panelists for this guideline development are nuclear medicine specialists who are representatives from Nuclear Medicine Society of Thailand (S.T., T.K., B.Kh., W.C., T.T., N.W., Ch.C., and P.K.), medical physicists/technologists from Thai Medical Physicist Society (P.P., T.S., N.P, and S.A.), and neurologists from The Neurological Society of Thailand and Dementia Association of Thailand (Y.L. and V.S.). The guideline development process is shown in Scheme 1.

The flow of imaging investigation in dementia syndrome is shown in Scheme 2, and the summarized implications of nuclear medicine investigations in dementia syndrome with the level of evidence are listed below in Table 2 [12–34].

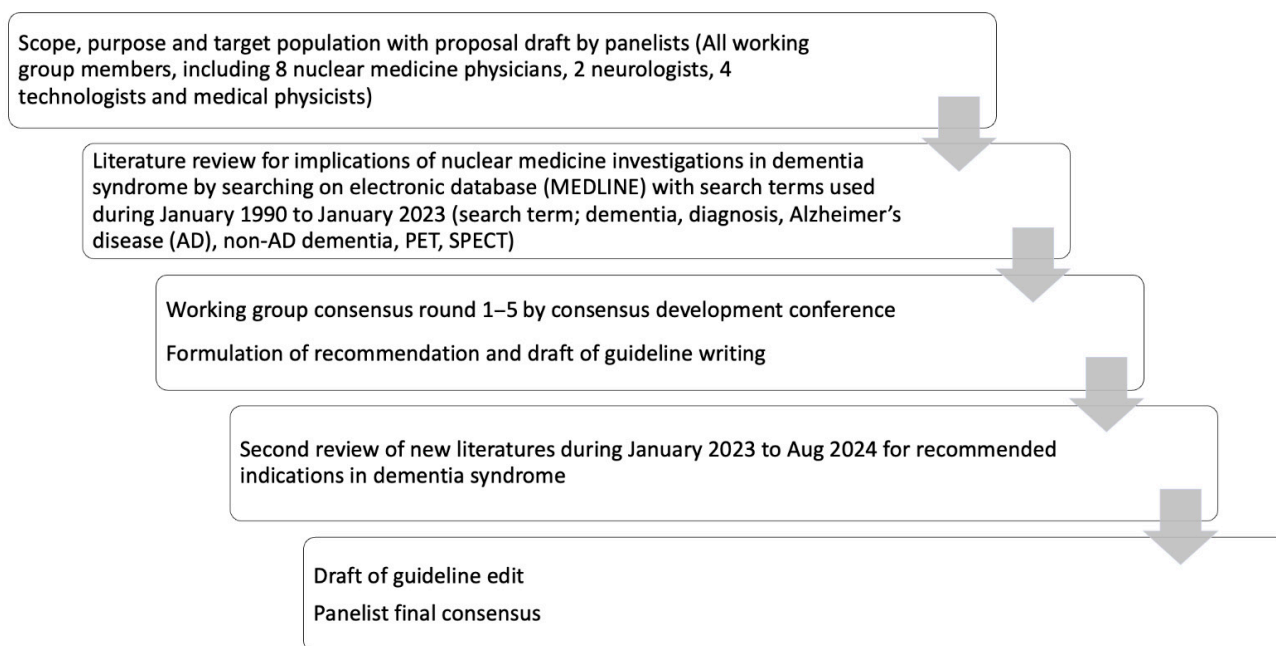
Table 2. Indications for PET and SPECT in dementia syndrome.

| Investigations | Implication for Clinical Practice | Level of Evidence |
|---|-----------------------------------|-------------------|
| To predict AD dementia conversion | | |
| FDG PET | ++ | I [12,13] |
| Brain perfusion SPECT | + | I [13] |
| Amyloid PET | ++ | I [14–16] |
| Tau PET (use with amyloid PET) | + | I [15] |
| To support early-onset Alzheimer’s disease (EOAD) diagnosis | | |

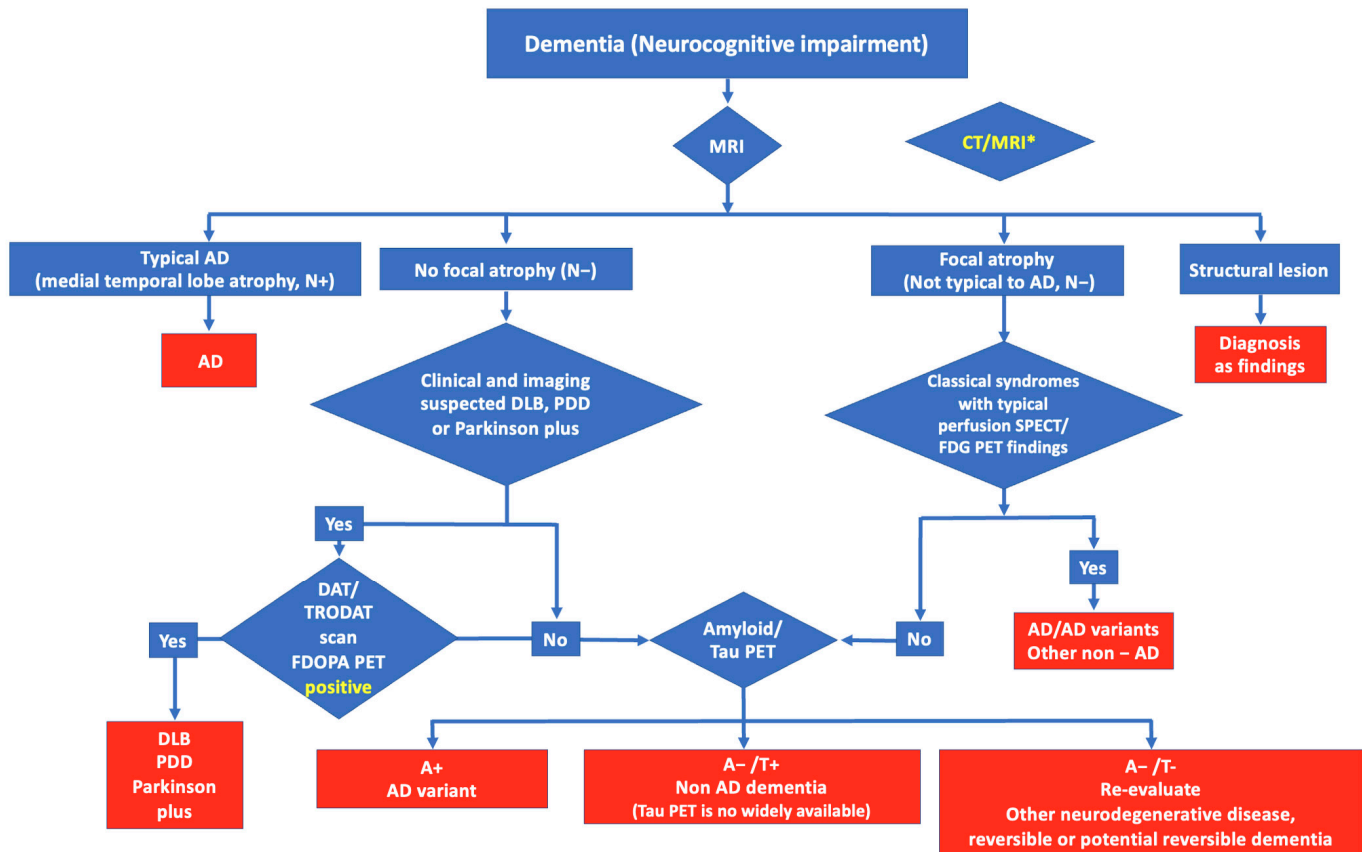
Table 2. Cont.

| Investigations | Implication for Clinical Practice | Level of Evidence |
|---|-----------------------------------|----------------------|
| FDG PET | ++ | I [17–19] |
| Brain perfusion SPECT | + | II [20,21] |
| Amyloid PET | ++ | I [17,22–25] |
| Tau PET | + | I [25] II [26–30] |
| To differential diagnosis of AD variants | | |
| FDG PET | ++ | I [17,19] |
| Brain perfusion SPECT | + | II [20,21] |
| Amyloid PET | ++ | I [17,22–24] |
| Tau PET | + / – | II [27–30] |
| To differential diagnosis of AD vs. non-AD dementia | | |
| FDG PET | ++ | I [17,22,23,29] |
| Brain perfusion SPECT | + | II [31,32] |
| Amyloid PET | ++ | I [18,19,28,30] |
| Tau PET | + | III [20,21,24,27] |
| To differential diagnosis of LBD vs. non-LBD | | |
| FDG PET | ++ | I [33] |
| Brain perfusion SPECT | + | I [33] II [34] |
| DAT SPECT | ++ | II [12,35] |
| MIBG scan | ++ | II [12] |
| Tau PET (differentiate DLB and PCA) | ++ | II [12] |

Note: ++ clinically useful investigation; + possibly useful investigation; + / – investigational;. Levels of evidence: Level I: High-quality prospective cohort study with adequate power or systematic review of these studies; Level II: Lesser quality prospective cohort, retrospective cohort study, untreated controls from an RCT, or systematic review of these studies; Level III: Case–control study or systematic review of these studies; Level IV: Case series; Level V: Expert opinion; case report or clinical example; or evidence based on physiology, bench research, or “first principles”.



Scheme 1. Guideline development process.



Scheme 2. The flow of nuclear medicine investigations in dementia syndrome. MRI = Magnetic resonance imaging; CT = Computed tomography; SPECT = Single-photon emission computed tomography; FDG PET = ¹⁸F-Fluorodeoxyglucose positron emission tomography; FDOPA PET = ¹⁸F-Fluoro-L-dopa positron emission tomography; AD = Alzheimer’s disease; DLB = Dementia with Lewy bodies; PDD = Parkinson’s disease dementia; A = Amyloid; T = Tau; N = Neurodegeneration. Note: * = CT is optional if MRI is not available.

Relative contraindications for nuclear medicine investigations are pregnancy/breastfeeding and the patients who are unable to cooperate.

5. Nuclear Medicine Imaging Procedures

5.1. Patient Preparation

The patient preparation for nuclear medicine investigations in dementia syndrome is shown in Table 3 [36–40].

Table 3. Patient preparation for brain perfusion SPECT and brain PET.

| | |
|-----------------------|---|
| Brain perfusion SPECT | <ol style="list-style-type: none"> 1. Review clinical history, physical examination, and anatomical images. 2. Advise the patient to avoid stimulants affecting cerebral blood flow: <ol style="list-style-type: none"> a. Caffeine, cola, alcohol, and energy drinks; b. Smoking. |
|-----------------------|---|

Table 3. *Cont.*

| | | |
|-----------------------------|----|---|
| FDG PET | 1. | Review clinical history, physical examination, and anatomical images. |
| | 2. | Fast for at least 4 h. |
| | 3. | Advise the patient to stop taking brain stimulants and drugs, as follows: <ol style="list-style-type: none"> Caffeine, cola, alcohol, and energy drinks; Smoking and excessive exercise; Stop taking these drugs for 4–6 half-lives: cocaine, anesthetics (propofol, isoflurane, barbiturates), benzodiazepine, corticosteroids, anti-psychotics (haloperidol, chlorpromazine), and cholinesterase inhibitors (donepezil, rivastigmine). |
| | 4. | On the acquisition day, blood glucose must be checked, and the optimal blood glucose level should not exceed 160 mg/dL. If blood glucose exceeds 200 mg/dL, rescheduling should be considered. Good hydration is advised. |
| | 5. | During the FDG injection and uptake period, place the patient in a quiet, dimly lit room with eyes open and ears unplugged. |
| | 6. | Sedation can be used if needed with short-acting benzodiazepines, such as midazolam, just before image acquisition. |
| | 7. | Continuously monitor vital signs and pulse oximetry during acquisition. |
| Amyloid and Tau PET imaging | 1. | Review clinical history, physical examination, and anatomical images |
| | 2. | No drug is advised to be withdrawn. |
| | 3. | Fasting is advised for at least 4 h to prepare for sedation if needed. |

5.2. Recommended Radiopharmaceutical Dosage

The recommended radiopharmaceutical dosage is shown in Table 4 [36–44].

Table 4. Radiopharmaceutical dosage.

| Radiopharmaceuticals | Dose |
|--|--|
| ^{99m}Tc HMPAO | 555–1110 MBq (15–30 mCi) Typical: 740 MBq (20 mCi) |
| ^{99m}Tc ECD | 555–1110 MBq (15–30 mCi) Typical: 1110 MBq (30 mCi) |
| ^{18}F -FDG | 185–740 MBq (5–20 mCi) |
| Amyloid imaging | |
| - ^{18}F -Florbetapir | 370 MBq (10 mCi) |
| - ^{18}F -Flutemetamol | 185 MBq (5 mCi) |
| - ^{18}F -Florbetaben | 300 MBq (8 mCi) |
| - ^{11}C -PiB | 300–370 MBq (8–10 mCi) |
| Tau tracer | |
| - ^{18}F -PI2620 | 185–300 MBq (5–8 mCi) |
| - ^{18}F -AV1451 | 370 MBq (10 mCi) |
| Variability in injected dose recommendation is based on differences in absorbed dose | |

5.3. Radiation Dosimetry

Radiation dosimetry in SPECT [36,37] and PET studies [39,41–46] is shown in Tables 5 and 6, respectively.

Table 5. Radiation dosimetry in SPECT studies.

| Agent | Dose in MBq Unit (mCi) | Organ Receiving the Highest Dose mGy/MBq | Effective Dose mSv/MBq |
|-------------------------|------------------------|--|------------------------|
| ^{99m} Tc HMPAO | 555–1110 (15–30) | 0.034 (kidney) | 0.0093 mSv |
| ^{99m} Tc ECD | 555–1110 (15–30) | 0.05 (bladder wall) | 0.0077 |

Table 6. Radiation dosimetry in PET/CT studies in adults.

| Agent | Dose in MBq Unit (mCi) | Organ Receiving the Highest Dose mGy/MBq | Effective Dose mSv/MBq |
|------------------------------|------------------------|--|------------------------|
| ¹⁸ F-FDG | 185–740 (5–20) | 0.13 (bladder wall) | 0.019 |
| ¹⁸ F-Florbetapir | 370 MBq (10 mCi) | 0.143 (gallbladder wall) | 0.019 |
| ¹⁸ F-Flutemetamol | 185 MBq (5 mCi) | 0.287 (gallbladder wall) | 0.034 |
| ¹⁸ F-Florbetaben | 300 MBq (8 mCi) | 0.137 (gallbladder wall) | 0.019 |
| ¹¹ C-PiB | 300 MBq (8 mCi) | 44.80 ± 29.30 (gallbladder wall) | 5.3 |
| ¹⁸ F-PI2620 | 185–300 MBq | N/A | N/A |
| ¹⁸ F-AV1451 | 370 MBq | N/A | 0.024 |

N/A: Data not available.

5.4. Brain Perfusion SPECT Acquisition and Image Reconstruction Parameter

The brain perfusion SPECT and SPECT/CT acquisition and reconstruction parameters are shown in Table 7 [37,47].

Table 7. SPECT and SPECT/CT acquisition and reconstruction parameters.

| Agent | Waiting Time after Injection | Acquisition Time (min) |
|---------------------------|--|------------------------|
| ^{99m} Tc ECD | 15 min–6 h (optimum at 45 min) | 30 |
| ^{99m} Tc HMPAO | 30 min–6 h (optimum at 90 min) | 30 |
| Instrument | SPECT | |
| Collimator | Fan beam or parallel hole (LEHR/LEUHR) * | |
| Energy setting | 140 keV, 15–20% energy window | |
| Zoom | To gain at least a pixel size equal to 1/3 to 1/2 of the expected resolution | |
| Nuclide | ^{99m} Tc | |
| Matrix Size | ≥128 × 128 | |
| Scan mode | Step and shoot or continuous | |
| Rotation per view | ≤3° (total of 360° rotation) | |
| Time per view | About 15–30 s/projection (total count 5 × 10 ⁶ counts) | |
| Scatter correction | Optional | |
| Reconstruction | 3D-OSEM **/FBP | |
| Slice thickness | Possible 3–5 mm (for maximal pixel resolution) | |
| (if SPECT/CT) | Scout/Surview/Topogram CT (optional in some vendors) | |
| CT voltage | 120–140 kV | |
| CT current | ≤30 mA | |
| (if SPECT/CT) | CT (for attenuation correction) | |

Table 7. Cont.

| Agent | Waiting Time after Injection | Acquisition Time (min) |
|---|---------------------------------|------------------------|
| (if SPECT/CT) | CT (for attenuation correction) | |
| CT voltage | 120–140 kV | |
| CT current | ≤80 mA | |
| Slice thickness | 3–5 mm | |
| Acquisition steps for an individual patient | | |
| <ul style="list-style-type: none"> - Lie supine with arms down on the machine table. - Immobilize the head to reduce movement. - Center the head in the field of view. - Hold the head straight without tilting in the canthomeatal line perpendicular to the detector. - Use the smallest radius of rotation as much as possible or use an automated contour setting from the patient to the detector to ensure maximal image resolution. | | |
| SPECT processing | | |
| <ul style="list-style-type: none"> - Review of projection data in cine mode and sonogram for an initial determination of image quality, patient motion, and artifacts. - Reconstruct by ordered subset expectation maximization (OSEM) or filtered back projection (FBP) algorithm. - Select the type of low pass filter, i.e., Butterworth, Hamming or Hanning. - Optimize reconstructing parameters, i.e., cut-off, order, iterations, and subset, depending on the injected activity, resolution, and camera sensitivity. - Use either calculated (e.g., Chang's method) or measured (e.g., Gadolinium source or CT scan) attenuation for attenuation correction. - Apply scatter correction (optional) to improve image signal-to-noise ratio. The most popular one is triple-energy-window correction. | | |

* Low-energy high resolution (LEHR) or low-energy ultra high resolution (LEUHR); ** Ordered subsets expectation maximization (OSEM) or filtered back projection (FBP); SPECT = Single-photon emission computed tomography; CT = Computed tomography; AC = Attenuation correction; keV = Kiloelectronvolt; sec = Second; mm = Millimeter; kV = Kilovolt; mA = Milliampere.

5.5. PET Acquisition and Image Reconstruction Parameter

The brain PET acquisition and reconstruction parameters are shown in Table 8 [38–40,48,49].

Table 8. PET/CT acquisition and reconstruction parameters.

| Scout or Survivew CT | |
|--|---|
| CT voltage | 120 kV |
| CT current | ≤30 mA |
| CT | |
| Scan type | Helical |
| Rotation time | 0.75–1 s |
| Matrix | 512 |
| Slice thickness (mm) | 3–5 mm |
| Slice increments | continuous |
| Pitch | ≤1 |
| CT voltage | 120–140 kV |
| CT current.time | ≤50 mAs (Low dose CT), ≤250 mAs (diagnostic CT) |
| PET | |
| Energy setting | 511 keV, 15–20% energy window |
| Glucose metabolic radiopharmaceutical and dose | ¹⁸ F-Fluorodeoxyglucose (FDG) 185–740 MBq (5–20 mCi) |
| Amyloid radiopharmaceutical and dose | ¹⁸ F-Florbetapir 370 MBq (10 mCi) |
| | ¹⁸ F-Flutemetamol 185 MBq (5 mCi) |
| | ¹⁸ F-Florbetaben 300 MBq (8 mCi) |
| | ¹¹ C-PiB 300 MBq (8 mCi) |

Table 8. Cont.

| Scout or Surview CT | |
|--|--|
| Tau radiopharmaceutical and dose | ¹⁸ F-PI-2620 185–300 MBq (5–8 mCi) ¹⁸ F-AV1451 370 MBq (10 mCi) |
| Uptake time | ¹⁸ F-FDG 30–60 min ¹⁸ F-Florbetapir 30–50 min ¹⁸ F-Flutemetamol 60–120 min ¹⁸ F-Florbetaben 45–130 min ¹¹ C-PiB 40–70 min ¹⁸ F-PI2620 30–75 min ¹⁸ F-AV1451 80 min |
| Mode | 3D |
| Scan direction | Toward head |
| Scan Duration (min/bed) | ¹⁸ F-FDG 5–30 min ¹⁸ F-Florbetapir 10 min ¹⁸ F-Flutemetamol 10–20 min ¹⁸ F-Florbetaben 15–20 min ¹¹ C-PiB 40–70 min ¹⁸ F-PI2620 45 min (5 min per frame) ¹⁸ F-AV1451 20 min |
| Attenuation correction | Yes (use CT) |
| Scatter correction | Yes |
| Reconstruction | Iterative (OSEM) |
| Acquisition steps for an individual patient | |
| <ul style="list-style-type: none"> - Lie supine with arms down on the machine table. - Set the patient's head in a holder in the center of the field of view with the canthomeatal line in the vertical position. - Immobilize the head to reduce movement. | |
| PET processing | |
| <ul style="list-style-type: none"> - Preview images for patient motion and ensure PET and CT images are matched before performing CT attenuation correction. - Images are reconstructed in the transaxial plane of 128 × 128 (for semiquantitative analysis) or preferably 256 × 256 matrix size or more for better image resolution. - Typical transaxial pixel size is 2–3 mm and slice thickness is 2–4 mm. - A final image resolution may vary between 2.5 and 10 mm full-width at half maximum (FWHM), depending on the resolution of the PET system. - The reconstruction parameters can be varied. Please refer to the manufacturer's recommendations for the best choices of iterations, subsets, and smoothness. | |

PET = Positron emission tomography; CT = Computed tomography; AC = Attenuation correction; keV = Kiloelectronvolt; sec = Second; mm = Millimeter; kV = Kilovolt; mA = Milliampere; min = Minute.

6. Imaging Data Display, Image Interpretation, and Reporting Format

6.1. Brain Perfusion SPECT and FDG PET

6.1.1. Imaging Data Display [45,50]

The display plane for SPECT and PET is the AC–PC plane (parallel to the line passing from the anterior commissure to the posterior commissure, which is approximately the line passing through the anterior and posterior poles of the brain in a sagittal image).

Resliced axial images are usually used for interpretation, while coronal and sagittal images help to better delineate abnormal regions.

A continuous gray or color display scheme could be selected according to the reader's preference.

The surface projection technique with comparison to a normal age-matched database by Z-score using three-dimensional stereotactic surface projections (3D-SSP) or Neurostat further avoids misdiagnosis of dementia type made by visual analysis alone. It improves diagnostic confidence for brain perfusion SPECT and FDG-PET, especially in non-experienced

readers [51,52]. Other programs, such as eZIS [53] that compare the patient's data with or without a normal database can also be used depending on the user's preferences.

Three-dimensional stereotactic surface projection (3D-SSP) is software for neurological image analysis, which compares a patient's brain to an age-matched normal database voxel-by-voxel with normalization of the count to the brain region that is usually not affected by the disease process, e.g., thalamus, cerebellum, and pons. Global brain (whole gray matter) for reference is optional.

The easy Z-score imaging system, or eZIS [53], combines statistical parametric mapping (SPM) and 3D-SSP. Instead of using a normal database for robust statistical imaging analysis, eZIS can utilize SPM processing in normalization, smoothing, and image conversion functions for statistical analysis. Furthermore, if a normal database is available, even from different institutes or different cameras/SPECTs, it can also be used.

Examples of brain perfusion SPECT and brain FDG-PET image display for visual analysis in Alzheimer's disease are demonstrated in Figures 1 and 2, respectively.

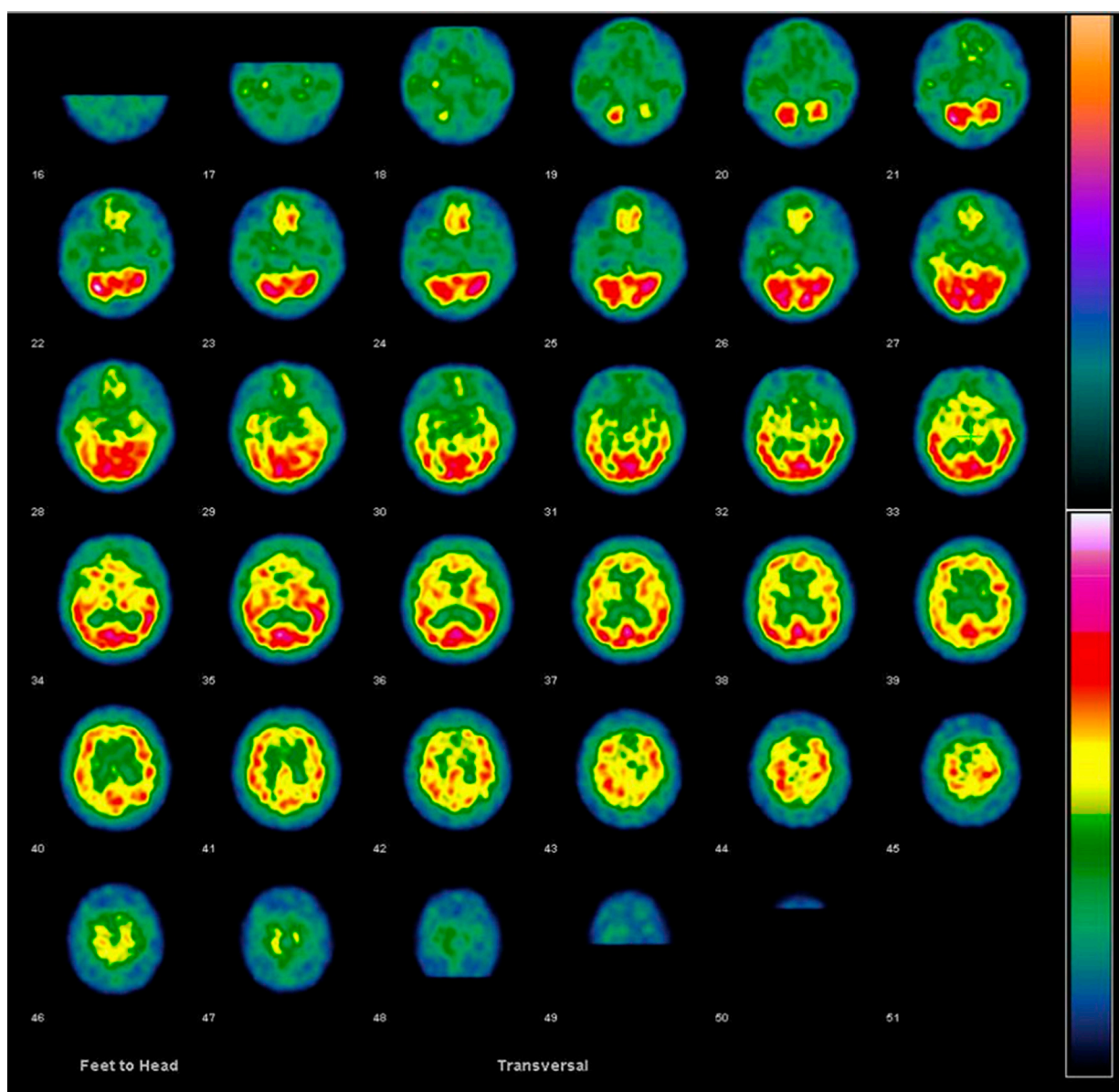


Figure 1. Brain ECD SPECT in frontotemporal dementia displayed in rainbow color scale in the axial AC-PC plane.

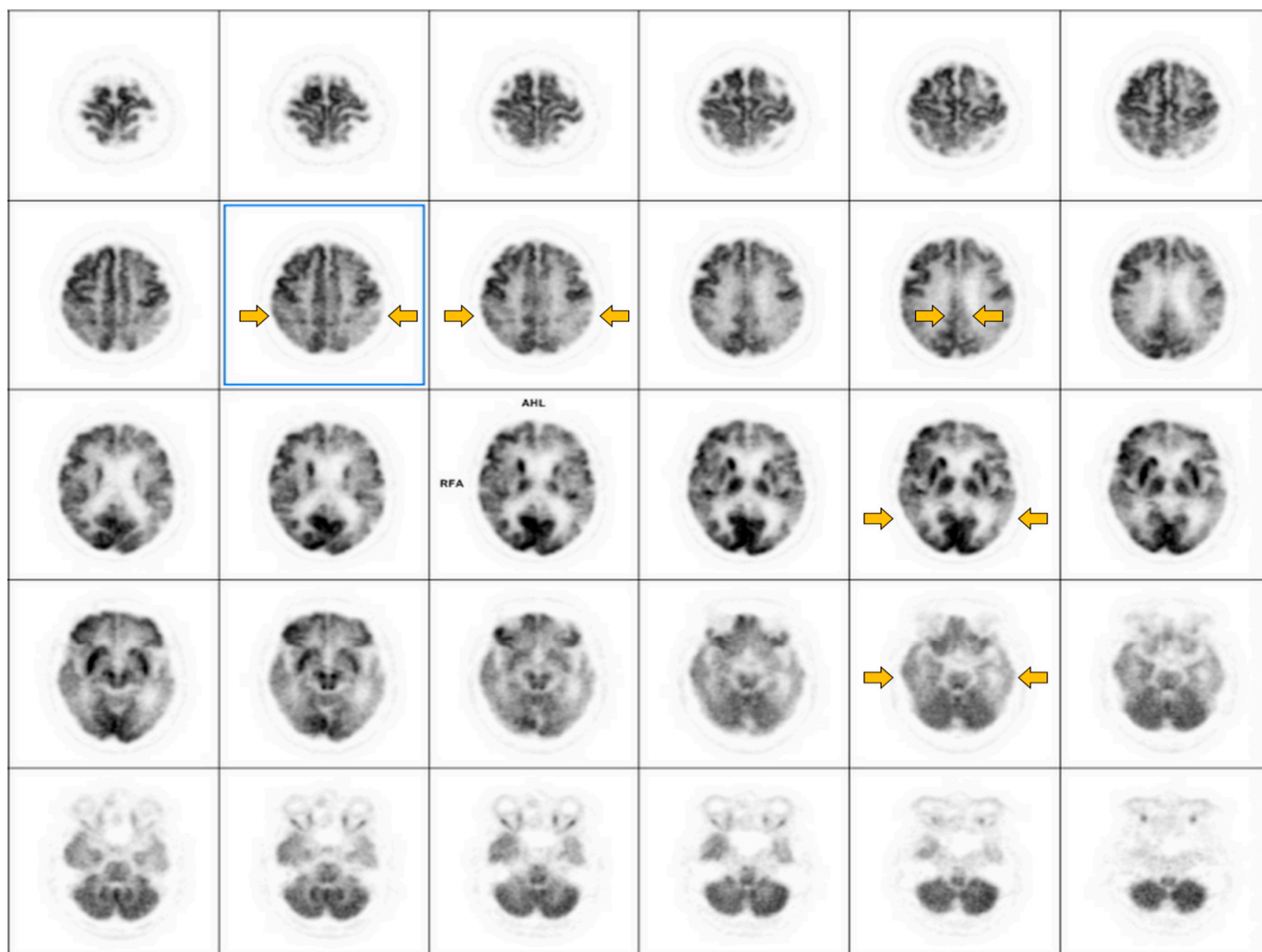


Figure 2. Brain FDG-PET in Alzheimer’s disease displayed in the axial AC–PC plane. Hypometabolism at posterior cingulate gyri, precuneus, bilateral parietal and temporal cortices (yellow arrows), with relatively preserved metabolism at bilateral primary sensorimotor areas, visual cortices, basal ganglia, thalami, and cerebelli are observed. (Black shows higher metabolism and gray to white show lower metabolism).

6.1.2. Image Interpretation for Brain Perfusion SPECT and FDG-PET

Since brain perfusion tracers, e.g., ^{99m}Tc ECD and brain glucose metabolism PET radiopharmaceutical (^{18}F -FDG), are taken up by neuronal cells, depending on synaptic activity [54–56], their uptake thus also represents areas of viable cells. Dementia, which has synaptic dysfunction and neuronal death, can be imaged with these two types of imaging. Areas of hypoperfusion/hypometabolism are the areas to look for in dementia. Each type of dementia shows specific patterns of hypoperfusion/hypometabolism in the cortex, as shown in Table 9 [57–63].

Using 3D-SSP, the hypometabolic regions affected in each type of dementia are more evident, as shown in Figure 3.

Table 9. Specific hypoperfusion/hypometabolic patterns in each type of dementia.

| Dementia Type | Hypoperfusion/Metabolic Cortical and Subcortical Regions | Preservation of Perfusion/Metabolism |
|--|--|---|
| Alzheimer’s disease (AD) | <ul style="list-style-type: none"> - Posterior cingulate gyri, precunei, parietal lobes, and superior/posterior temporal lobes (can be asymmetric) - Frontal lobes in advanced cases AD variants (more predominate in hypoperfusion/hypometabolic region) - Frontal variant (fvAD): orbitofrontal, medial frontal - Logopenic variant primary progressive aphasia (lvPPA): left temporoparietal predominate, extending toward more anterior temporal cortex - Posterior cortical atrophy (PCA): bilateral parieto-occipital lobes (usually right predominate) ± frontal eye field | <ul style="list-style-type: none"> - Primary sensory-motor cortices - Primary visual cortices - Basal ganglia, thalami |
| Dementia with Lewy bodies (DLB) | <ul style="list-style-type: none"> - Similar findings to AD plus primary visual cortex | <ul style="list-style-type: none"> - Posterior cingulate gyri (relatively preserved cingulate island sign) |
| Frontotemporal lobar degeneration (FTLD) | <ul style="list-style-type: none"> - Frontal and anterior temporal lobes - FTLD variants (more predominate in hyperperfusion/hypometabolic region): <ul style="list-style-type: none"> - Behavioral variant (bvFTD): medial prefrontal - Semantic (SD): anterior temporal lobes - Progressive non-fluent aphasia (PNFA): pre-Rolandic left lateral and medial frontal | <ul style="list-style-type: none"> - Posterior cingulate |
| Vascular dementia | <ul style="list-style-type: none"> - Various locations in cortical and subcortical gray matter and cerebellum | |

Note: Correlation with anatomical imaging for interpretation is recommended.

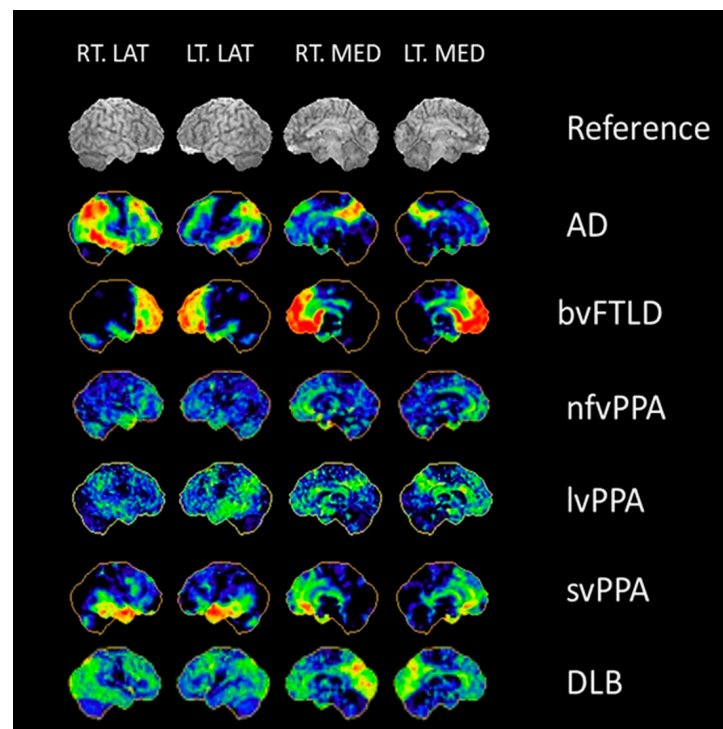


Figure 3. 3D-SSP of dementia syndrome. Courtesy: Professor Satoshi Minoshima, modified with permission. LT = left, RT = right, LAT = lateral view, MED = medial view, AD = Alzheimer’s disease,

bvFTLD = behavioral variant FTD, nfvPPA = non-fluent variant primary progressive aphasia, lvPPA = logopenic variant primary progressive aphasia, svPPA = semantic variant primary progressive aphasia, DLB = dementia with Lewy bodies. Color shows the specific hypometabolic brain region in each type of dementia.

6.1.3. Reporting Format

Each report must include specific details, such as the patient's identification, the referring clinician, the date and time of the study, and the reporting physician's signature for quality assurance purposes. The reporting physician must ensure these details are accurately matched with the main content of the report. The suggested structure for reports on brain SPECT and brain PET [36,37,45,64,65] consists of four key sections.

- History: The relevant history should be noted along with an indication of the study, for example, clinical cognitive impairment and other related disorders, type of suspected dementia, duration of symptom, recent medication, and findings of other related studies (e.g., neuropsychological test, CT, and MRI).
- Techniques:
 1. Radiopharmaceutical type and dosage.
 2. Uptake time: after tracer injection to image acquisition.
 3. Describe imaging and processing techniques, including imaging quality and limitations. These should also be thoroughly detailed if specific software or anatomical co-registration methods are used.
 4. Ancillary drugs (if used), e.g., type and time of sedative drugs.
 5. Fasting duration and serum glucose level for FDG PET.
 6. Type of additional software, e.g., 3D-SSP and normal age range and ethnicity, used for analysis.
- Findings:
 - a. SPECT or PET hypoperfusion/hypometabolic regions should be mentioned. Its location, extension, and severity should be reported.
 - b. Semiquantitative results (if done) e.g., Z-score comparison, can be described.
 - c. Correlative imaging findings, if available, e.g., MRI and CT, should be mentioned
- Interpretations/Impressions/Conclusions: Conclude whether the hypoperfusion/hypometabolic pattern found matches with the type of dementia. The final impression from imaging data should be interpreted along with available clinical and correlative imaging data. If they seem discordant, direct discussion with the multidisciplinary team would be the best (if possible) or provide further recommendations.

6.2. Brain Amyloid PET

6.2.1. Imaging Data Display [39]

The pixel size of at least 16-bit pixels.

Imaging plane: The alignment for displaying the tomographic images is the AC-PC line. The transaxial images are mainly used for image interpretation. However, coronal and sagittal images are also helpful in differentiating the distribution of the radiotracer in gray matter from subcortical white matter and confirming that the entire brain has been reviewed.

The color scale should be specific for the radiopharmaceutical used, as follows:

Gray scale: ^{18}F -florbetaben

Color (Rainbow): ^{11}C -PiB, ^{18}F -flutemetamol and ^{18}F -NAV4694

Reverse gray scale: ^{18}F -florbetapir

Maximum intensity of the display scale

^{18}F -florbetapir: the brightest region of overall brain uptake

^{18}F -florbetaben: the white matter maximum

¹⁸F-flutemetamol: setting the scale intensity in the pons region to 90%

6.2.2. Image Interpretation for Brain Amyloid PET

Visual Analysis [39,66–68]

There are different criteria for interpreting amyloid PET images among radiotracers, and interpreters should know the recommendations specific to a given amyloid tracer (Table 10). However, there are fundamental principles that can be applied. A systematic review of transaxial amyloid PET images starts at the cerebellar level. Usually, the cerebellar cortices are free from beta-amyloid deposition. Therefore, this level references normal cortical activity and gray–white matter contrast. After that, it is recommended to scroll up to review the entire cerebral cortical and subcortical regions with particular attention to the frontal, lateral temporal, posterior cingulate/precuneus, parietal cortices, and the basal ganglia. The visual analysis comprises a binary interpretation as a positive or negative scan.

Table 10. The recommended color scale and criteria for a positive scan use visual and semiquantitative analysis with the standardized uptake value ratio (SUVR) for each radiopharmaceutical to assess beta-amyloid deposition.

| Radiopharmaceuticals | Color Scale | Criteria For Positive Scan | Cortical Region | SUVR Cut-Off for Positive Scan | Reference Region |
|------------------------------|----------------------------|--|--|--------------------------------|-------------------|
| ¹¹ C-PiB | Color (Rainbow) | Binding in GM > WM | N/A | 1.4–1.6 | Cerebellar cortex |
| ¹⁸ F-florbetapir | Black/white (Reverse gray) | Loss of GM/WM contrast > 1 region | Temporal > occipital > prefrontal > parietal | 1.1–1.34 | Whole cerebellum |
| ¹⁸ F-flutemetamol | Color (Rainbow) | Increased GM uptake or loss of GM/WM contrast > 4 cortical and 1 subcortical regions | Frontal > posterior cingulate/precuneus > insula > temporal > striatum | 0.58–0.62 | Pons |
| ¹⁸ F-florbetaben | Black/white (Gray) | Increased GM uptake extending to the cortical margin > 4 cortical regions | Lateral temporal > frontal > posterior cingulate > parietal | 1.43 | Cerebellar cortex |
| ¹⁸ F-NAV4694 | Color (Rainbow) | N/A * | N/A * | 1.4–1.5 | Cerebellar cortex |

* N/A = not available (but similar criteria as in ¹¹C-PiB are assumed); Apart from visual and quantification analyses, as previously mentioned, there are several ongoing studies on using artificial intelligence (AI), which is beyond the scope of the current guidelines.

Negative Scan

Normal distribution for beta-amyloid radiopharmaceuticals is predominantly in the white matter with no or little retention in the gray matter. With the clear distinction of radiotracer uptake between gray and white matter, there is a nicely seen contrast between gray and white matter. In ¹¹C-PiB, some radiotracer uptake within the cerebral cortices can be expected but not exceed that in the adjacent white matter. The mechanism of white matter uptake is considered non-specific and varies among radiotracers. The negative uptake pattern resembles a blueprint of white matter distribution, i.e., a white matter sulcal pattern, with numerous concave arboreal ramifications. There should be a clear, wide, irregular gap between the cerebral hemispheres. Example images of negative scans are shown in Figure 4.

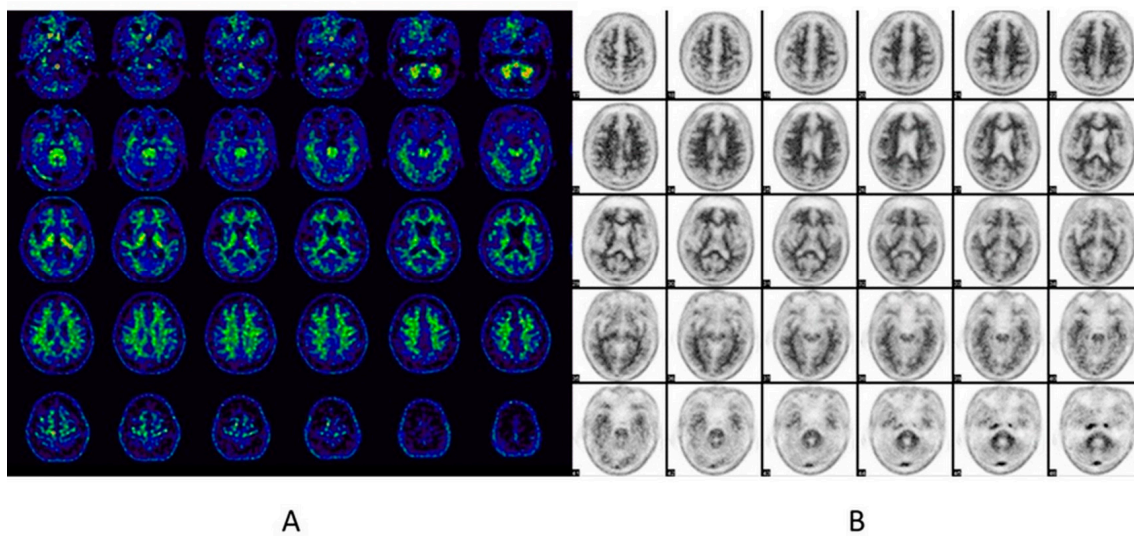


Figure 4. Example images of negative scans for beta-amyloid deposition acquired from (A) ^{11}C -PiB and (B) ^{18}F -florbetapir.

Positive Scan

A positive scan is defined as increased retention of tracer radiopharmaceutical uptake in the cerebral cortices, with the same or higher intensity as compared to the uptake in the white matter, and it forms a smooth, regular boundary. The typical brain regions involved are the frontal cortex, medial and lateral posterior parietal cortices, precuneus, occipital cortex, lateral temporal cortices, and striatum (most notably at the caudate head). By contrast, the sensorimotor and visual cortex can be relatively preserved. A typical finding in a positive ^{11}C -PiB scan is the intense retention in the cerebral cortices (cortical ribbon), which is higher than in the white matter. This finding is less often seen in ^{18}F -labeled radiopharmaceuticals, which is generally considered a positive scan when loss of the normal white matter pattern or loss of the gray matter and white matter contrast. Example images of negative scans are shown in Figure 5. However, there are differences in details regarding the criteria used to define amyloid positivity among radiopharmaceuticals. The brief criteria for brain amyloid positivity for each radiopharmaceutical are summarized in Table 10.

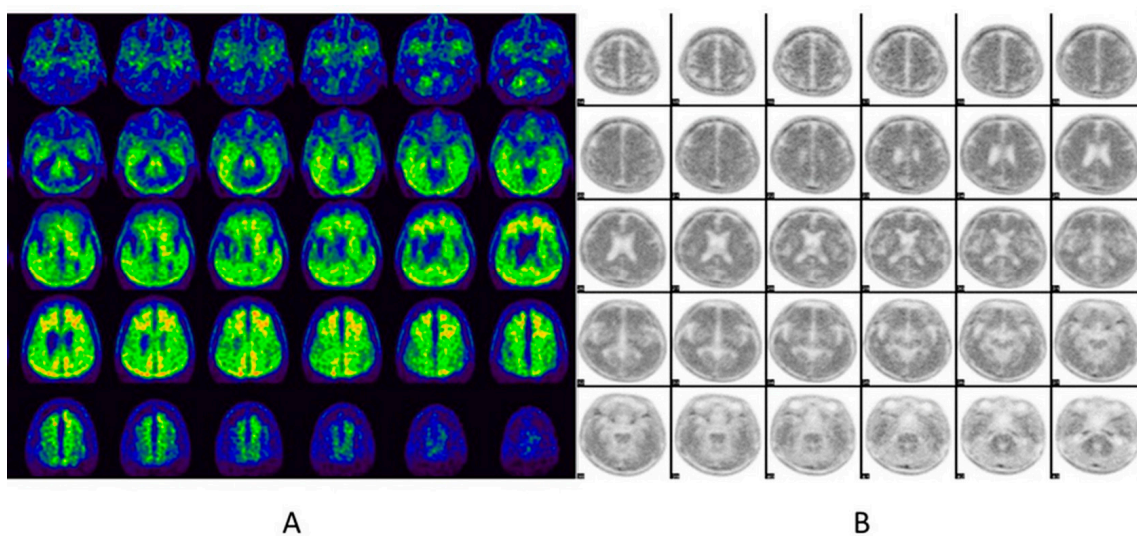


Figure 5. Example images of positive scans for beta-amyloid deposition acquired from (A) ^{11}C -PiB and (B) ^{18}F -florbetapir.

Please note that positive amyloid PET can be found in other conditions apart from Alzheimer's disease, including dementia with Lewy bodies (DLB), Parkinson's disease dementia (PDD), and cerebral amyloid angiopathy (CAA). In the elderly population with normal cognition, the incidence of amyloid positivity also increases with age [69,70].

In some complex cases, the available CT or fused PET/CT images or coregistration of PET and MRI images can provide helpful information on localization (gray vs. white matter) of radiotracer uptake. Structural MRI also potentially contributes to the differential diagnosis of dementia type, both in amyloid PET positive and negative cases [71,72].

Quantification

Quantification analysis to obtain numeric data of amyloid PET images can support visual analysis objectively, assess temporal change, and compare individual PET results with those of the normal control population. Absolute quantitative measurements of amyloid tracer deposition using a dynamic PET imaging protocol and tracer kinetic analysis are not required clinically but may be used for research. However, some semiquantitative analytical methods, namely the SUVR, Centiloid scale, and 3D-SSP, can be performed using available computer-aided analysis software for the clinic.

a. Standardized uptake value ratio (SUVR)

The SUVR is a semiquantitative analysis determined by the ratio between the SUV of the cortical region of interest divided by the SUV of the specific reference region recommended for each radiopharmaceutical. Several cortical brain regions are used to assess the SUVR: the global cerebral cortex, frontal, temporal, parietal, precuneus, anterior/posterior cingulate, and composite region, which combines several regional cortices. The brain regions suggested as reference regions are known to be spared from beta-amyloid deposition, either cerebellum (whole or cortex) or pons. However, the cut-off value of the SUVR for amyloid positivity has yet to be agreed upon [68,73,74].

b. Centiloid scale (CL) [75–78]

The Centiloid scale was proposed to overcome the limitation of using different radiopharmaceuticals to assess beta-amyloid deposition across centers, which makes it difficult for comparison purposes and in multicenter research trials. The concept of this quantification method is to translate the SUVR in the same regions of the brain obtained from each radiopharmaceutical into the common number, called the Centiloid, which ranges from 0 to 100, using the standard formula created from the previous research to assess the association between regional SUV data from each radiopharmaceutical and reference radiopharmaceutical (^{11}C -PiB). The average SUVR from cortical VOIs to be used for calculating the CL value are the frontal combination (consisting of dorsolateral prefrontal, ventrolateral prefrontal, and orbitofrontal regions), superior parietal, lateral temporal, lateral occipital, anterior/posterior cingulate, and precuneus.

The example formulas for calculating the Centiloid value generated for each radiopharmaceutical are as follows. However, the formula may vary depending on the data and the processing pipeline (e.g., SPM vs. PMOD vs. FSL Centiloid method) [78]. An example of cortical VOIs of beta-amyloid PET images coregistered with MRI is shown in Figure 6.

- (1) $CL_{\text{PiB}} = 93.7 \times \text{SUVR} - 94.6$
- (2) $CL_{\text{florbetapir}} = 175.43 \times \text{SUVR} - 182.26$
- (3) $CL_{\text{flutemetamol}} = 119.53 \times \text{SUVR} - 118.57$
- (4) $CL_{\text{florbetaben}} = 153.4 \times \text{SUVR} - 154.9$
- (5) $CL_{\text{NAV4694}} = 85.32 \times \text{SUVR} - 87.97$

Recent data with ^{11}C -PiB and ^{18}F -florbetaben using brain autopsy results as a gold standard found that a CL value < 10 accurately suggested no neuritic plaque, a CL value > 20 suggested at least moderate plaque density, and a CL value of 50 or more best confirmed both neuropathological and clinicopathological diagnosis of AD [79].

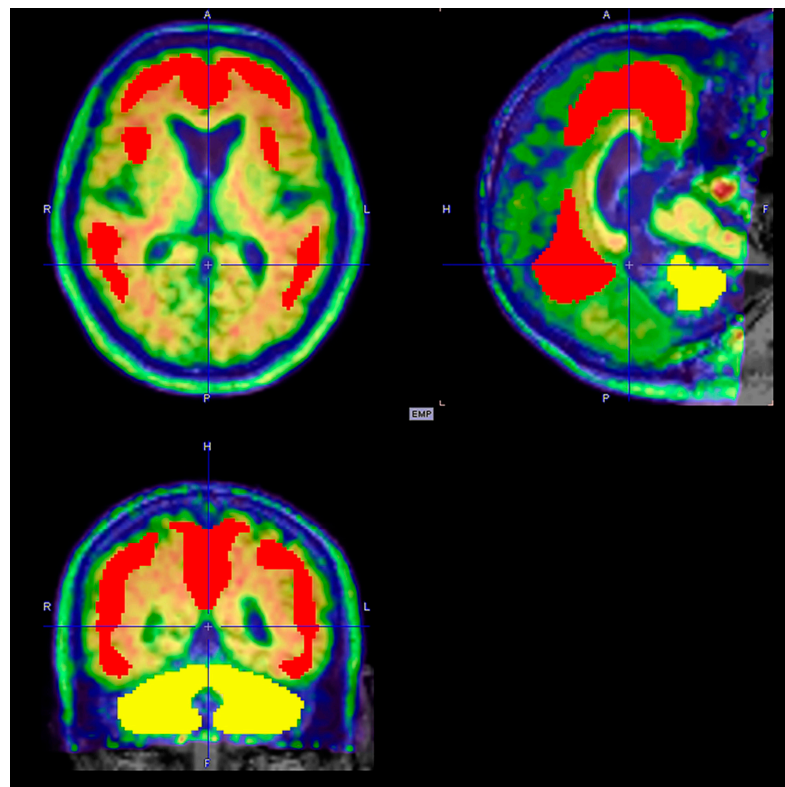


Figure 6. Example of cortical VOIs (red) of beta-amyloid PET images co-registered with the MRI template for assessing the composite SUVR with the whole cerebellum (yellow) as the reference region. The SUVR will be used to calculate the Centiloid scale. Automatic calculation of the Centiloid scale has recently been available in some software packages (courtesy of Assistant Professor Chakmeedaj Sethanandha, Siriraj Hospital, Mahidol University).

c. Three-dimensional stereotactic surface projection (3D-SSP) [80,81]

The 3D-SSP technique is used for assessing the difference in radiotracer activity in the brain in comparison with a normal database. The differences are displayed as Z-score and Z-score map images (Figure 7). This technique has been widely used with many radiopharmaceuticals, although the data in amyloid PET are still relatively limited [82,83].

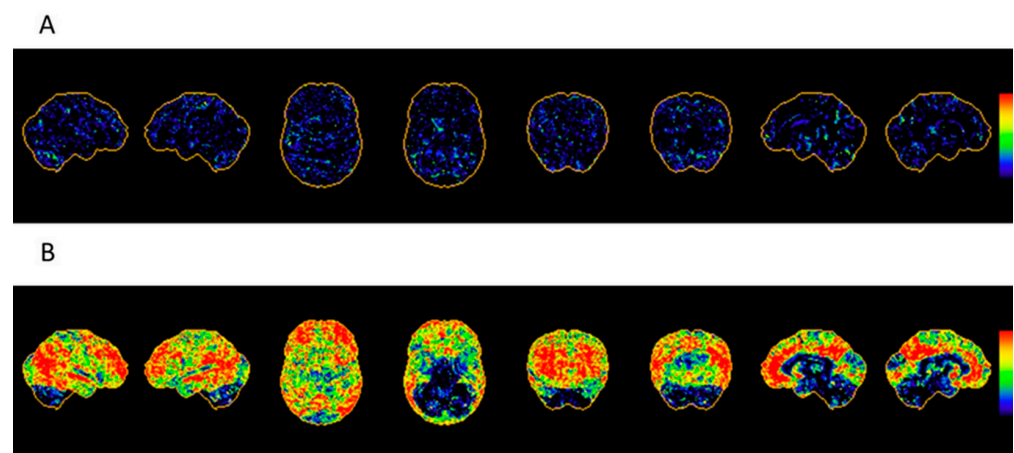


Figure 7. Examples of 3D-SSP Z-score map images from ^{18}F -florbetapir PET scans in (A) normal elderly with negative amyloid deposition and (B) patients with Alzheimer's disease and positive amyloid deposition. The 3D-SSP Z-score: Black represents negative amyloid deposition, progressively increasing deposition from blue to red on the color bar.

6.2.3. Reporting Format

Specific identification of each patient, the referring clinician, date and time of the study, and the reporting physician's signature must be provided in the report as part of quality assurance. The responsibility of the reporting physician is to match this part to the body of the report correctly. The recommended structural body of the report includes four significant portions, as follows:

- History: The relevant history should be described along with an indication of the study. The specific clinical symptoms of MCI or dementia and the reasons for the test (e.g., atypical age of onset, uncertain clinical diagnoses, known comorbidities, or potential candidate for clinical trial) should be briefly documented.
- Techniques:
 1. Radiopharmaceutical type and dosage.
 2. Injection to imaging interval of radiopharmaceutical.
 3. Detailed imaging and processing techniques should be mentioned, including imaging quality and limitations. If certain specific software or anatomical co-registration is utilized, it should be additionally detailed.
 4. Type of additional software used for quantification analysis, e.g., 3D-SSP, SPM, PMOD, FreeSurfer, Hermes, MIMneuro, NeuroQ, or other commercially available or vendor-specific software
- Findings:
 - a. Visual analysis: The pattern of radiotracer distribution in the bilateral white matter and cerebellum should be discussed. The gray–white matter contrast should be mentioned, and the affected lobe with a loss of gray–white matter contrast should be noted. Abnormal radiotracer uptake in the cerebral cortices or cerebellar cortices, either the same degree and more intense than the white matter uptake, if any, should be described. If present, the degree and location of cerebral atrophy should also be mentioned.
 - b. Quantification analysis (optional): Describe the method used to obtain quantification data (SUVR or Centiloid scale) and the results.
- Interpretations/Impressions/Conclusions: Negative/positive brain PET scan for beta-amyloid deposition (absence/presence of significant beta-amyloid deposition in the brain).

Note: Indeterminate or inconclusive results should be reported with possible reasons, such as technical or physiological factors. The report should not state amyloid positivity as the diagnostic of Alzheimer's disease [39,66].

Evidence-based:

Previous data revealed comparable sensitivity and specificity among different radiopharmaceuticals in differentiating patients with Alzheimer's disease from normal controls [66,80,81]. The overall sensitivity and specificity of ¹⁸F-labeled amyloid tracers by visual analysis (pooled sensitivity of 90% and specificity of 82–95%) and quantification methods (pooled sensitivity of 90% and specificity of 83–94%) are also comparable. The pooled sensitivity of PiB PET is slightly higher (96%) but with lower specificity (58%) [24].

The recently reviewed data from several studies on the clinical utility of amyloid PET imaging in dementia disorders found that this technique is potentially proper on change of diagnosis in 29%, gain of diagnostic confidence in 63%, change of medication in 38%, and overall change of management in 64% of cases. The diagnostic confidence of referring physicians also increased by approximately 20% with amyloid PET results [84]. The management effect of amyloid PET in terms of change of diagnosis was also higher when the scan was performed under AUC (62.4%) than when a non-AUC scan was performed (45.2%) [85]. The impact of amyloid imaging on patient outcomes is still under investigation.

6.3. Tau PET

Tau is a protein that has the role of stabilization in the microtubules in neurons, predominantly within axons. If abnormality occurs, tau protein is hyperphosphorylated, which causes it to lose the function of binding to microtubules and then aggregate into neurofibrillary tangles (NFTs), leading to loss of cell function and cell death [86]. Hyperphosphorylated tau has six isoforms, which can be divided into two functional groups based on the number of repeated microtubule-binding domains [3R and 4R] [87].

Tauopathies are neurodegenerative disorders characterized by abnormal tau protein deposition in the brain, resulting in clinical syndromes [88]. Primary tauopathies constitute a significant class of frontotemporal lobar degeneration (FTLD) neuropathy and can have several presentations, such as frontotemporal dementia (FTD) [i.e., behavioral variant FTD, primary progressive aphasia], progressive supranuclear palsy (PSP), and corticobasal degeneration (CBD). In Alzheimer's disease (AD), the primary pathology includes neurofibrillary tau neuropathy in addition to amyloid-beta ($A\beta$) and is considered a secondary or non-primary tauopathy (Table 11) [89–91].

Table 11. Histopathological appearance of tau isoforms and conformation in different tauopathies.

| Tauopathy | Histopathology | | Tau Isoform |
|----------------------------------|---------------------|---|-------------|
| | Electron Microscope | Light Microscope | |
| Primary tauopathies | | | |
| Progressive supranuclear palsy | SF (and TF) | Tufted astrocytes; globose tangles | 4R |
| Corticobasal degeneration | SF (and TF) | Astrocytic plaques | 4R |
| Argyrophilic grain disease | SF | Oligodendroglial coiled bodies; limbic argyrophilic grains | 4R |
| Pick's disease | TF (and SF) | Pick's bodies | 3R |
| Myotonic dystrophy | N/A | Neurofibrillary tangles | Short 0N3R |
| Secondary tauopathies | | | |
| Alzheimer's disease | PHF (and SF) | Neurofibrillary tangles | 3R and 4R |
| Down syndrome | PHF (and SF) | Neurofibrillary tangles | 3R and 4R |
| Chronic traumatic encephalopathy | PHF (and SF) | Neurofibrillary tangles | 3R and 4R |
| Niemann-Pick disease type C | PHF (and SF) | Neurofibrillary tangles | 3R and 4R |

3R: three repeated; 4R: four repeated; PHF: paired helical filaments; SF: straight filaments; TF: twisted filaments; N/A: data not available. Short 0N3R: the shortest isoform of fetal tau (where N denotes the number of N-terminal inserts and R is the number of microtubule-binding domains).

In AD, neurofibrillary tangles (NFTs) are a key characteristic. The quantity of NFTs is linked to the severity of AD, indicating a stronger association with neuronal dysfunction compared to amyloid imaging. According to the Braak AD staging, NFTs initially appear in the perirhinal and entorhinal cortex (stage I), then in the CA1 region of the hippocampus (stage II). They subsequently accumulate in the limbic structures, including the hippocampus (stage III) and the amygdala, thalamus, and claustrum (stage IV). In the advanced stages, NFTs spread throughout the neocortex, with earlier and more severe impacts on specific areas (stage V) before affecting the primary sensory, motor, and visual regions (stage VI). Therefore, a tau pathology biomarker is a promising tool for diagnosing AD. In contrast to Alzheimer's disease, there is still limited data for tau accumulation in the non-AD tauopathy group. However, some studies are showing that CBS patients have higher uptake in the putamen, globus pallidus, and subthalamic nucleus [92], and PSP patients also show significantly higher uptake in the subcortical brain region, especially in the globus pallidus but not in the dorsal midbrain [93].

For tau imaging, there are several types of tau radiopharmaceuticals, e.g., quinolone derivative (^{18}F -THK 523, ^{18}F -THK 5117, ^{18}F -THK 5351), benzothiazole derivative (^{11}C -PBB3), and benzimidazole derivative (^{18}F -AV1451) [94]. However, the first generation of tau radiopharmaceuticals had high off-target binding to monoamine oxidase enzyme. Thus, the second generation was developed. Among the second generation of tau radiopharmaceuticals, 18F-PI2620 has been used in Thailand. 18F-PI2620 has been proven to have a high binding affinity to phosphorylated tau (both 3R and 4R isoforms) with absent off-target binding in AD and non-AD tauopathies [46,95].

6.3.1. Imaging Data Display

PET images are automatically co-registered with each individual, using an automatic voxel of interest (VOI) based on the maximum probability following the automated anatomical labeling (AAL)-merged atlas. PET images are then registered to the T1-MRI. The standardized uptake value ratio (SUVR) of ^{18}F -PI-2620 is analyzed for various brain regions, using the cerebellar gray matter (excluding the vermis and anterior lobe surrounding the vermis) as the reference region [48]. The processed images are displayed with the color scale in the axial view along the anterior commissure—posterior commissure line (AC–PC line), coronal view, and sagittal view.

6.3.2. Image Interpretation for Tau PET

Visual Analysis

The normal population has no specific area of ^{18}F -PI-2620 cerebral uptake visually. However, variable uptake of the skull may be generally seen. Suppose there is tau accumulation in cortical regions, mainly at the temporal and parietal lobe, precuneus, and posterior cingulate cortex. The study will be interpreted as positive, as shown in Figure 8 [46,48].

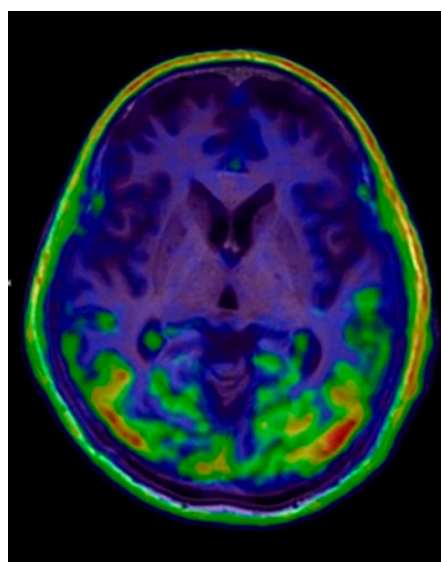


Figure 8. Positive tau PET: A fused ^{18}F -PI2620 PET/T1-weight MRI image shows increased ^{18}F -PI-2620 uptake at the inferior temporal, occipital, and parietal cortices and no off-target binding at the basal ganglia.

Quantitative Analysis

Quantitation using the SUVR is still limited for ^{18}F -PI-2620 due to the small number of patients, unintended patient movement in later time frames, and small brain volume in some regions. Thus, the SUVR should be interpreted along with visual analysis [48].

6.3.3. Reporting Format

- History: Indication, the patient's clinical presentation, and correlative imaging.
- Techniques: Imaging is performed on an integrated 64-slice PET/CT scanner for the whole brain, with non contrast-enhanced CT for attenuation correction and localization in the transaxial, coronal, and sagittal planes. A 3D emission dynamic scan of the same area is acquired in a one-bed position. Semiquantitative calculations are performed using PMOD software with the automatic anatomical labeling (AAL)-merged atlas to generate automatic voxels of interest for different brain regions.
- Findings: Visual analysis: Describe abnormal tau deposition in the brain region.
- Interpretations/Impressions/Conclusions: Negative/positive studies should be mentioned when reporting the region of abnormal tau deposition.

Note: Imaging data should be interpreted along with available data from clinical context and correlative imaging.

7. Pitfalls

Many biological and technical factors affect image interpretation, as shown in Table 12 [38,40,47,96].

Table 12. Pitfalls and Errors.

| Perfusion SPECT | |
|--|--|
| Biological factors | Technical factors |
| <ol style="list-style-type: none"> Unintended brain activity from external stimuli Interference effect on cerebral blood flow, e.g., sedative drug Anatomical variations | <ol style="list-style-type: none"> Misregistration artifact Inappropriate processing, e.g., the reconstruction method Non-continuous color and inappropriate plane of the image display Level of contrast and background subtraction Partial volume effect on the corrected image |
| FDG PET | |
| Biological factors | Technical factors |
| <ol style="list-style-type: none"> Unintended brain activity from external stimuli Interference effect on cerebral glucose metabolism, e.g., sedative drug or high serum glucose level Recent radio- or chemotherapy Brain glucose metabolic alteration due to the aging process | <ol style="list-style-type: none"> Misregistration artifact Inappropriate processing, e.g., reconstruction method Non-continuous color and inappropriate plane of the image display Level of contrast and background subtraction Partial volume effect on the corrected image |
| Amyloid and Tau PET | |
| Biological factors | Technical factors |
| <ol style="list-style-type: none"> Aging Cortical atrophy Encephalomalacia Extracerebral activity Non-specific uptake in the white matter and skull Off-target binding of tau tracer | <ol style="list-style-type: none"> Partial volume artifact Motion artifact Low dose of tracer injection Delayed scan time Under-smooth reconstruction |

8. Radiation Exposure Risk Concern and Management

In nuclear medicine imaging for dementia, managing radiation doses is essential, especially in older patients. Although SPECT generates slightly more radiation than PET, risks are minimal for a single scan but can accumulate with multiple imaging sessions. PET, on the other hand, generally provides less radiation exposure than SPECT with more detailed images. Thus, it is valuable in repeated imaging. To mitigate the risk, clinicians should balance diagnostic needs with exposure risks. On the nuclear medicine side, it is recommended to use minimum effective tracer doses and consider alternatives like PET/MRI to reduce radiation further. Nuclear imaging radiation doses are generally low, but optimizing protocols helps to minimize cumulative risk while providing essential diagnostic insight.

9. Conclusions and Future Direction

The scope of applicability for these guidelines is aimed at hospitals with nuclear medicine departments. Since SPECT is generally more accessible and cost-effective compared to PET, SPECT can help to differentiate dementia subtypes (e.g., Alzheimer’s disease vs. vascular dementia) using perfusion tracers. In complex cases in which the diagnosis is still questionable, referring to higher-level centers with PET to perform specific tracers for Alzheimer’s pathology, such as amyloid and tau imaging, is recommended for more accurate dementia subtype differentiation. Tailoring the use of SPECT and PET in dementia diagnosis based on the hospital level could ensure both cost-effectiveness and optimal patient care across various healthcare settings.

In the near future, PET/MRI could become more prominent for their ability to simultaneously provide metabolic and structural insights. New tracers targeting amyloid, tau, and

other proteins could allow for even earlier and more precise diagnosis. Machine learning for SPECT and PET image analysis holds promise for improved accuracy in dementia subtype differentiation and disease progression tracking.

Author Contributions: Conceptualization, S.T. and T.K.; literature review and rated recommendation for indications in nuclear medicine imaging, Y.L., V.S., S.T., and T.K.; nuclear medicine imaging procedure, radiopharmaceuticals, and interpretation, S.T., B.K., T.K., W.C., T.T., N.W., C.C., P.K., P.P., T.S., N.P.-i., and S.A.; pitfalls and errors, B.K., T.K., and T.T.; original draft preparation, T.K. and S.T.; writing review and editing, T.K. and S.T. All authors have read and agreed to the published version of the manuscript.

Funding: This research received no external funding.

Acknowledgments: The authors thank Satoshi Minoshima and Chakmeedj Sethanandha for permission to use the figures.

Conflicts of Interest: The authors declare no conflicts of interest.

References

- Gale, S.A.; Acar, D.; Daffner, K.R. Dementia. *Am. J. Med.* **2018**, *131*, 1161–1169. [[CrossRef](#)] [[PubMed](#)]
- Murphy, M.P.; Levine, H., III. Alzheimer's Disease and The Amyloid-Beta Peptide. *J. Alzheimer's Dis.* **2010**, *19*, 311–323. [[CrossRef](#)] [[PubMed](#)]
- Deture, M.A.; Dickson, D.W. The Neuropathological Diagnosis of Alzheimer's Disease. *Mol. Neurodegener.* **2019**, *14*, 32. [[CrossRef](#)]
- Rawat, P.; Sehar, U.; Bisht, J.; Selman, A.; Culbertson, J.; Reddy, P.H. Phosphorylated Tau in Alzheimer's Disease and Other Tauopathies. *Int. J. Mol. Sci.* **2022**, *23*, 12841. [[CrossRef](#)]
- Hyman, B.T.; Phelps, C.H.; Beach, T.G.; Bigio, E.H.; Cairns, N.J.; Carrillo, M.C.; Montine, T.J. National Institute on Aging–Alzheimer's Association guidelines for the neuropathologic assessment of Alzheimer's disease. *Alzheimer's Dement.* **2012**, *8*, 1–13. [[CrossRef](#)] [[PubMed](#)]
- Montine, T.J.; Phelps, C.H.; Beach, T.G.; Bigio, E.H.; Cairns, N.J.; Dickson, D.W.; Hyman, B.T. National institute on Aging–Alzheimer's Association guidelines for the neuropathologic assessment of Alzheimer's disease: A practical approach. *Acta Neuropathol.* **2012**, *123*, 1–11. [[CrossRef](#)]
- Dickerson, B.; Atri, A. Molecular Imaging Biomarkers in Dementia: Amyloid and tau PET imaging aids evaluation of patients suspected of having Alzheimer disease or other dementias. *Pract. Neurol.* **2020**, *19*, 34–45.
- Young, P.N.E.; Estarellas, M.; Coomans, E.; Srikrishna, M.; Beaumont, H.; Maass, A.; Venkataraman, A.V.; Lissaman, R.; Jiménez, D.; Betts, M.J.; et al. Imaging biomarkers in neurodegeneration: Current and future practices. *Alzheimer's Res. Ther.* **2020**, *12*, 49. [[CrossRef](#)]
- American Psychiatric Association. Diagnostic and statistical manual of mental disorders. *Am. Psychiatric Assoc.* **2013**, *21*, 591–643.
- Petersen, R.C.; Smith, G.E.; Waring, S.C.; Ivnik, R.J.; Tangalos, E.G.; Kokmen, E. Mild cognitive impairment: Clinical characterization and outcome. *Arch. Neurol.* **1999**, *56*, 303–308. [[CrossRef](#)]
- Sachdev, P.S.; Blacker, D.; Blazer, D.G.; Ganguli, M.; Jeste, D.V.; Paulsen, J.S.; Petersen, R.C. Classifying neurocognitive disorders: The DSM-5 approach. *Nat. Rev. Neurol.* **2014**, *10*, 634–642. [[CrossRef](#)] [[PubMed](#)]
- Cotta Ramusino, M.; Massa, F.; Festari, C.; Gandolfo, F.; Nicolosi, V.; Orini, S.; Nobili, F.; Frisoni, G.B.; Morbelli, S.; Garibotto, V. Diagnostic performance of molecular imaging methods in predicting the progression from mild cognitive impairment to dementia: An updated systematic review. *Eur. J. Nucl. Med. Mol. Imaging* **2024**, *51*, 1876–1890. [[CrossRef](#)] [[PubMed](#)]
- Zhu, L.; Zhao, W.; Chen, J.; Li, G.; Qu, J. Systematic review and meta-analysis of diagnostic test accuracy (DTA) studies: The role of cerebral perfusion imaging in prognosis evaluation of mild cognitive impairment. *Ann. Palliat. Med.* **2022**, *11*, 673–683. [[CrossRef](#)] [[PubMed](#)]
- Ruan, D.; Sun, L. Amyloid- β PET in Alzheimer's disease: A systematic review and Bayesian meta-analysis. *Brain Behav.* **2023**, *13*, e2850. [[CrossRef](#)]
- Huszár, Z.; Engh, M.A.; Pavlekovics, M.; Sato, T.; Steenkamp, Y.; Hanseeuw, B.; Terebessy, T.; Molnár, Z.; Hegyi, P.; Csukly, G. Risk of conversion to mild cognitive impairment or dementia among subjects with amyloid and tau pathology: A systematic review and meta-analysis. *Alzheimer's Res. Ther.* **2024**, *16*, 81. [[CrossRef](#)]
- Chen, X.; Li, M.; Wang, S.; Zhu, H.; Xiong, Y.; Liu, X. Pittsburgh compound B retention and progression of cognitive status—A meta-analysis. *Eur. J. Neurol.* **2014**, *21*, 1060–1067. [[CrossRef](#)]
- McKhann, G.M.; Knopman, D.S.; Chertkow, H.; Hyman, B.T.; Jack, C.R., Jr.; Kawas, C.H.; Klunk, W.E.; Koroshetz, W.J.; Manly, J.J.; Mayeux, R.; et al. The diagnosis of dementia due to Alzheimer's disease: Recommendations from the National Institute on Aging–Alzheimer's Association workgroups on diagnostic guidelines for Alzheimer's disease. *Alzheimer's Dement.* **2011**, *7*, 263–269. [[CrossRef](#)] [[PubMed](#)]
- Bloudek, L.M.; Spackman, D.E.; Blankenburg, M.; Sullivan, S.D. Review and meta-analysis of biomarkers and diagnostic imaging in Alzheimer's disease. *J. Alzheimer's Dis.* **2011**, *26*, 627–645. [[CrossRef](#)]

19. Ou, Y.N.; Xu, W.; Li, J.Q.; Guo, Y.; Cui, M.; Chen, K.L.; Huang, Y.Y.; Dong, Q.; Tan, L.; Yu, J.T. FDG-PET as an independent biomarker for Alzheimer's biological diagnosis: A longitudinal study. *Alzheimer's Res. Ther.* **2019**, *11*, 57. [[CrossRef](#)]
20. Talbot, P.R.; Lloyd, J.J.; Snowden, J.S.; Neary, D.; Testa, H.J. A clinical role for ^{99m}Tc-HMPAO SPECT in the investigation of dementia? *J. Neurol. Neurosurg. Psychiatry* **1998**, *64*, 306–313. [[CrossRef](#)]
21. Valotassiou, V.; Malamitsi, J.; Papatriantafyllou, J.; Dardiotis, E.; Tsougos, I.; Psimadas, D.; Alexiou, S.; Hadjigeorgiou, G.; Georgoulas, P. SPECT and PET imaging in Alzheimer's disease. *Ann. Nucl. Med.* **2018**, *32*, 583–593. [[CrossRef](#)] [[PubMed](#)]
22. Clark, C.M.; Schneider, J.A.; Bedell, B.J.; Beach, T.G.; Bilker, W.B.; Mintun, M.A.; Pontecorvo, M.J.; Hefti, F.; Carpenter, A.P.; Flitter, M.L.; et al. Use of florbetapir-PET for imaging beta-amyloid pathology. *JAMA* **2011**, *305*, 275–283. [[CrossRef](#)] [[PubMed](#)]
23. Joshi, A.D.; Pontecorvo, M.J.; Clark, C.M.; Carpenter, A.P.; Jennings, D.L.; Sadowsky, C.H.; Adler, L.P.; Kovnat, K.D.; Seibyl, J.P.; Arora, A.; et al. Performance characteristics of amyloid PET with florbetapir F 18 in patients with Alzheimer's disease and cognitively normal subjects. *J. Nucl. Med. Off. Publ. Soc. Nucl. Med.* **2012**, *53*, 378–384. [[CrossRef](#)] [[PubMed](#)]
24. Morris, E.; Chalkidou, A.; Hammers, A.; Peacock, J.; Summers, J.; Keevil, S. Diagnostic accuracy of ¹⁸F amyloid PET tracers for the diagnosis of Alzheimer's disease: A systematic review and meta-analysis. *Eur. J. Nucl. Med. Mol. Imaging* **2016**, *43*, 374–385. [[CrossRef](#)]
25. Cho, H.; Mundada, N.S.; Apostolova, L.G.; Carrillo, M.C.; Shankar, R.; Amuiri, A.N.; Zeltzer, E.; Windon, C.C.; Soleimani-Meigooni, D.N.; Tanner, J.A.; et al. Amyloid and tau-PET in early-onset AD: Baseline data from the Longitudinal Early-onset Alzheimer's Disease Study (LEADS). *Alzheimer's Dement. J. Alzheimer's Assoc.* **2023**, *19* (Suppl. 9), S98–S114. [[CrossRef](#)]
26. Tanner, J.A.; Iaccarino, L.; Edwards, L.; Asken, B.M.; Gorno-Tempini, M.L.; Kramer, J.H.; Pham, J.; Perry, D.C.; Possin, K.; Malpetti, M.; et al. Amyloid, tau and metabolic PET correlates of cognition in early and late-onset Alzheimer's disease. *Brain A J. Neurol.* **2022**, *145*, 4489–4505. [[CrossRef](#)]
27. Cho, H.; Choi, J.Y.; Hwang, M.S.; Lee, J.H.; Kim, Y.J.; Lee, H.M.; Lyoo, C.H.; Ryu, Y.H.; Lee, M.S. Tau PET in Alzheimer disease and mild cognitive impairment. *Neurology* **2016**, *87*, 375–383. [[CrossRef](#)]
28. La Joie, R.; Visani, A.V.; Baker, S.L.; Brown, J.A.; Bourakova, V.; Cha, J.; Chaudhary, K.; Edwards, L.; Iaccarino, L.; Janabi, M.; et al. Prospective longitudinal atrophy in Alzheimer's disease correlates with the intensity and topography of baseline tau-PET. *Sci. Transl. Med.* **2020**, *12*, eaau5732. [[CrossRef](#)] [[PubMed](#)]
29. Cho, H.; Baek, M.S.; Lee, H.S.; Lee, J.H.; Ryu, Y.H.; Lyoo, C.H. Principal components of tau positron emission tomography and longitudinal tau accumulation in Alzheimer's disease. *Alzheimer's Res. Ther.* **2020**, *12*, 114. [[CrossRef](#)]
30. Koychev, I.; Gunn, R.N.; Firouzian, A.; Lawson, J.; Zamboni, G.; Ridha, B.; Sahakian, B.J.; Rowe, J.B.; Thomas, A.; Rochester, L.; et al. PET Tau and Amyloid- β Burden in Mild Alzheimer's Disease: Divergent Relationship with Age, Cognition, and Cerebrospinal Fluid Biomarkers. *J. Alzheimer's Dis.* **2017**, *60*, 283–293. [[CrossRef](#)]
31. Archer, H.A.; Smailagic, N.; John, C.; Holmes, R.B.; Takwoingi, Y.; Coulthard, E.J.; Cullum, S. Regional cerebral blood flow single photon emission computed tomography for detection of Frontotemporal dementia in people with suspected dementia. *Cochrane Database Syst. Rev.* **2015**, *6*, CD010896. [[CrossRef](#)]
32. Valotassiou, V.; Papatriantafyllou, J.; Sifakis, N.; Tzavara, C.; Tsougos, I.; Psimadas, D.; Kapsalaki, E.; Fezoulidis, I.; Hadjigeorgiou, G.; Georgoulas, P. Brain perfusion SPECT with Brodmann areas analysis in differentiating frontotemporal dementia subtypes. *Curr. Alzheimer Res.* **2014**, *11*, 941–954. [[CrossRef](#)] [[PubMed](#)]
33. O'Brien, J.T.; Firbank, M.J.; Davison, C.; Barnett, N.; Bamford, C.; Donaldson, C.; Olsen, K.; Herholz, K.; Williams, D.; Lloyd, J. ¹⁸F-FDG PET and perfusion SPECT in the diagnosis of Alzheimer and Lewy body dementias. *J. Nucl. Med. Off. Publ. Soc. Nucl. Med.* **2014**, *55*, 1959–1965. [[CrossRef](#)]
34. Chiba, Y.; Fujishiro, H.; Iseki, E.; Kasanuki, K.; Sato, K. The Cingulate Island Sign on FDG-PET vs. IMP-SPECT to Assess Mild Cognitive Impairment in Alzheimer's Disease vs. Dementia with Lewy Bodies. *J. Neuroimaging* **2019**, *29*, 712–720. [[CrossRef](#)]
35. McCleery, J.; Morgan, S.; Bradley, K.M.; Noel-Storr, A.H.; Ansorge, O.; Hyde, C. Dopamine transporter imaging for the diagnosis of dementia with Lewy bodies. *Cochrane Database Syst. Rev.* **2015**, *1*, CD010633. [[CrossRef](#)]
36. Juni, J.E.; Waxman, A.D.; Devous, M.D., Sr.; Tikofsky, R.S.; Ichise, M.; Van Heertum, R.L.; Carretta, R.F.; Chen, C.C. Procedure guideline for brain perfusion SPECT using ^{99m}Tc radiopharmaceuticals 3.0. *J. Nucl. Med. Technol.* **2009**, *37*, 191–195. [[CrossRef](#)]
37. Kapucu, Ö.L.; Nobili, F.; Varrone, A.; Booi, J.; Vander Borght, T.; Nägren, K.; Darcourt, J.; Tatsch, K.; Van Laere, K.J. EANM procedure guideline for brain perfusion SPECT using ^{99m}Tc-labelled radiopharmaceuticals, version 2. *Eur. J. Nucl. Med. Mol. Imaging* **2009**, *36*, 2093. [[CrossRef](#)] [[PubMed](#)]
38. Guedj, E.; Varrone, A.; Boellaard, R.; Albert, N.L.; Barthel, H.; van Berckel, B.; Brendel, M.; Cecchin, D.; Ekmekcioglu, O.; Garibotto, V.; et al. EANM procedure guidelines for brain PET imaging using [¹⁸F]FDG, version 3. *Eur. J. Nucl. Med. Mol. Imaging* **2022**, *49*, 632–651. [[CrossRef](#)] [[PubMed](#)]
39. Minoshima, S.; Drzezga, A.E.; Barthel, H.; Bohnen, N.; Djekidel, M.; Lewis, D.H.; Mathis, C.A.; McConathy, J.; Nordberg, A.; Sabri, O. SNMMI procedure standard/EANM practice guideline for amyloid PET imaging of the brain 1.0. *J. Nucl. Med.* **2016**, *57*, 1316–1322. [[CrossRef](#)]
40. Kaewchur, T.; Khiewvan, B.; Chamroonrat, W.; Lolekha, P.; Phokaewvarangkul, O.; Thientunyakit, T.; Wongsurawat, N.; Kiatkittikul, P.; Chotipanich, C.; Huang, W.-S.; et al. Thai national guideline for nuclear medicine investigation in movement disorders: Nuclear medicine society of Thailand, the neurological society of Thailand, and Thai medical physicist society collaboration. *Asia Ocean. J. Nucl. Med. Biol.* **2024**, *12*, 86–107. [[CrossRef](#)]

41. Silverman, D.H. Brain ¹⁸F-FDG PET in the diagnosis of neurodegenerative dementias: Comparison with perfusion SPECT and with clinical evaluations lacking nuclear imaging. *J. Nucl. Med. Off. Publ. Soc. Nucl. Med.* **2004**, *45*, 594–607.
42. Mormino, E.C.; Toueg, T.N.; Azevedo, C.; Castillo, J.B.; Guo, W.; Nadiadwala, A.; Corso, N.K.; Hall, J.N.; Fan, A.; Trelle, A.N.; et al. Tau PET imaging with ¹⁸F-PI-2620 in aging and neurodegenerative diseases. *Eur. J. Nucl. Med. Mol. Imaging* **2021**, *48*, 2233–2244. [[CrossRef](#)] [[PubMed](#)]
43. Klunk, W.E.; Engler, H.; Nordberg, A.; Wang, Y.; Blomqvist, G.; Holt, D.P.; Bergström, M.; Savitcheva, I.; Huang, G.F.; Estrada, S.; et al. Imaging brain amyloid in Alzheimer's disease with Pittsburgh Compound-B. *Ann. Neurol.* **2004**, *55*, 306–319. [[CrossRef](#)]
44. Mathis, C.A.; Mason, N.S.; Lopresti, B.J.; Klunk, W.E. Development of positron emission tomography β -amyloid plaque imaging agents. *Semin. Nucl. Med.* **2012**, *42*, 423–432. [[CrossRef](#)]
45. Varrone, A.; Asenbaum, S.; Vander Borght, T.; Booij, J.; Nobili, F.; Nagren, K.; Darcourt, J.; Kapucu, O.L.; Tatsch, K.; Bartenstein, P.; et al. EANM procedure guidelines for PET brain imaging using [¹⁸F]FDG, version 2. *Eur. J. Nucl. Med. Mol. Imaging* **2009**, *36*, 2103–2110. [[CrossRef](#)] [[PubMed](#)]
46. Mueller, A.; Bullich, S.; Barret, O.; Madonia, J.; Berndt, M.; Papin, C.; Perrotin, A.; Koglin, N.; Kroth, H.; Pfeifer, A.; et al. Tau PET imaging with ¹⁸F-PI-2620 in Patients with Alzheimer Disease and Healthy Controls: A First-in-Humans Study. *J. Nucl. Med.* **2020**, *61*, 911–919. [[CrossRef](#)] [[PubMed](#)]
47. Kaewchur, T.; Chamroonrat, W.; Thientunyakit, T.; Khiewvan, B.; Wongsurawat, N.; Chotipanich, C.; Chinvarun, Y.; Bunyaratavej, K.; Amnuaywattakorn, S.; Poon-Iad, N.; et al. Thai National Guideline for Nuclear Medicine Investigations in Epilepsy. *Asia Ocean. J. Nucl. Med. Biol.* **2021**, *9*, 188–206. [[CrossRef](#)] [[PubMed](#)]
48. Chotipanich, C.; Nivorn, M.; Kunawudhi, A.; Promteangtrong, C.; Boonkawin, N.; Jantarato, A. Evaluation of Imaging Windows for Tau PET Imaging Using ¹⁸F-PI2620 in Cognitively Normal Individuals, Mild Cognitive Impairment, and Alzheimer's Disease Patients. *Mol. Imaging* **2020**, *19*, 1536012120947582. [[CrossRef](#)] [[PubMed](#)]
49. Tian, M.; Civelek, A.C.; Carrio, I.; Watanabe, Y.; Kang, K.W.; Murakami, K.; Garibotto, V.; Prior, J.O.; Barthel, H.; Zhou, R.; et al. International consensus on the use of tau PET imaging agent ¹⁸F-flortaucipir in Alzheimer's disease. *Eur. J. Nucl. Med. Mol. Imaging* **2022**, *49*, 895–904. [[CrossRef](#)]
50. Waxman, A.D.; Herholz, K.; Lewis, D.H.; Herscovitch, P.; Minoshima, S.; Mountz, J.M.; Consensus GI, D. *Society of Nuclear Medicine Procedure Guideline for FDG PET Brain Imaging Version 1.0*; SNMMI: Reston, VA, USA, 2009.
51. Kim, J.; Cho, S.G.; Song, M.; Kang, S.R.; Kwon, S.Y.; Choi, K.H.; Choi, S.M.; Kim, B.C.; Song, H.C. Usefulness of 3-dimensional stereotactic surface projection FDG PET images for the diagnosis of dementia. *Medicine* **2016**, *95*, e5622. [[CrossRef](#)]
52. Ishii, K.; Ito, K.; Nakanishi, A.; Kitamura, S.; Terashima, A. Computer-assisted system for diagnosing degenerative dementia using cerebral blood flow SPECT and 3D-SSP: A multicenter study. *Jpn. J. Radiol.* **2014**, *32*, 383–390. [[CrossRef](#)]
53. Waragai, M.; Yamada, T.; Matsuda, H. Evaluation of brain perfusion SPECT using an easy Z-score imaging system (eZIS) as an adjunct to early-diagnosis of neurodegenerative diseases. *J. Neurol. Sci.* **2007**, *260*, 57–64. [[CrossRef](#)] [[PubMed](#)]
54. Buchert, R.; Santer, R.; Brenner, W.; Apostolova, I.; Mester, J.; Clausen, M.; Silverman, D.H. Computer simulations suggest that acute correction of hyperglycaemia with an insulin bolus protocol might be useful in brain FDG PET. *Nukl. Nucl. Med.* **2009**, *48*, 44–54.
55. Sokoloff, L. Localization of functional activity in the central nervous system by measurement of glucose utilization with radioactive deoxyglucose. *J. Cereb. Blood Flow. Metab. Off. J. Int. Soc. Cereb. Blood Flow. Metab.* **1981**, *1*, 7–36. [[CrossRef](#)]
56. Bentourkia, M.; Bol, A.; Ivanou, A.; Labar, D.; Sibomana, M.; Coppens, A.; Michel, C.; Cosnard, G.; De Volder, A.G. Comparison of regional cerebral blood flow and glucose metabolism in the normal brain: Effect of aging. *J. Neurol. Sci.* **2000**, *181*, 19–28. [[CrossRef](#)]
57. Small, G.W.; Bookheimer, S.Y.; Thompson, P.M.; Cole, G.M.; Huang, S.C.; Kepe, V.; Barrio, J.R. Current and future uses of neuroimaging for cognitively impaired patients. *Lancet. Neurol.* **2008**, *7*, 161–172. [[CrossRef](#)] [[PubMed](#)]
58. Lim, S.M.; Katsifis, A.; Villemagne, V.L.; Best, R.; Jones, G.; Saling, M.; Bradshaw, J.; Merory, J.; Woodward, M.; Hopwood, M.; et al. The ¹⁸F-FDG PET cingulate island sign and comparison to ¹²³I-beta-CIT SPECT for diagnosis of dementia with Lewy bodies. *J. Nucl. Med. Off. Publ. Soc. Nucl. Med.* **2009**, *50*, 1638–1645. [[CrossRef](#)]
59. Verfaillie, S.C.; Adriaanse, S.M.; Binnewijzend, M.A.; Benedictus, M.R.; Ossenkoppele, R.; Wattjes, M.P.; Pijnenburg, Y.A.; van der Flier, W.M.; Lammertsma, A.A.; Kuijter, J.P.; et al. Cerebral perfusion and glucose metabolism in Alzheimer's disease and frontotemporal dementia: Two sides of the same coin? *Eur. Radiol.* **2015**, *25*, 3050–3059. [[CrossRef](#)]
60. Jolepalem, P.; Wu, D. Semantic Dementia Diagnosed by F-18 FDG PET/MRI: Co-registered Images. *J. Clin. Imaging Sci.* **2013**, *3*, 35. [[CrossRef](#)]
61. Josephs, K.A.; Duffy, J.R.; Fossett, T.R.; Strand, E.A.; Claassen, D.O.; Whitwell, J.L.; Peller, P.J. Fluorodeoxyglucose F18 positron emission tomography in progressive apraxia of speech and primary progressive aphasia variants. *Arch. Neurol.* **2010**, *67*, 596–605. [[CrossRef](#)]
62. Harisankar, C.N.; Mittal, B.R.; Agrawal, K.L.; Abrar, M.L.; Bhattacharya, A.; Singh, B.; Modi, M. FDG-PET findings in fronto-temporal dementia: A case report and review of literature. *Indian. J. Nucl. Med. IJNM Off. J. Soc. Nucl. Med. India* **2011**, *26*, 96–98. [[CrossRef](#)]
63. Kerrouche, N.; Herholz, K.; Mielke, R.; Holthoff, V.; Baron, J.C. ¹⁸FDG PET in vascular dementia: Differentiation from Alzheimer's disease using voxel-based multivariate analysis. *J. Cereb. Blood Flow. Metab. Off. J. Int. Soc. Cereb. Blood Flow. Metab.* **2006**, *26*, 1213–1221. [[CrossRef](#)] [[PubMed](#)]

64. Yoshida, T.; Ha-Kawa, S.; Yoshimura, M.; Nobuhara, K.; Kinoshita, T.; Sawada, S. Effectiveness of treatment with donepezil hydrochloride and changes in regional cerebral blood flow in patients with Alzheimer's disease. *Ann. Nucl. Med.* **2007**, *21*, 257–265. [[CrossRef](#)] [[PubMed](#)]
65. Thomsen, G.; Knudsen, G.M. Procedure guideline for brain perfusion SPECT using ^{99m}Tc radiopharmaceuticals 3.0. *J. Nucl. Med. Technol.* **2010**, *38*, 209. [[CrossRef](#)]
66. Johnson, K.A.; Minoshima, S.; Bohnen, N.I.; Donohoe, K.J.; Foster, N.L.; Herscovitch, P.; Karlawish, J.H.; Rowe, C.C.; Carrillo, M.C.; Hartley, D.M. Appropriate use criteria for amyloid PET: A report of the Amyloid Imaging Task Force, the Society of Nuclear Medicine and Molecular Imaging, and the Alzheimer's Association. *J. Nucl. Med.* **2013**, *54*, 476–490. [[CrossRef](#)] [[PubMed](#)]
67. Schilling, L.P.; Zimmer, E.R.; Shin, M.; Leuzy, A.; Pascoal, T.A.; Benedet, A.L.; Borelli, W.V.; Palmieri, A.; Gauthier, S.; Rosa-Neto, P. Imaging Alzheimer's disease pathophysiology with PET. *Dement. Neuropsychol.* **2016**, *10*, 79–90. [[CrossRef](#)]
68. Rowe, C.C.; Villemagne, V.L. Brain amyloid imaging. *J. Nucl. Med. Technol.* **2013**, *41*, 11–18. [[CrossRef](#)]
69. Savva, G.M.; Wharton, S.B.; Ince, P.G.; Forster, G.; Matthews, F.E.; Brayne, C. Age, neuropathology, and dementia. *New Engl. J. Med.* **2009**, *360*, 2302–2309. [[CrossRef](#)]
70. Ossenkoppele, R.; Jansen, W.J.; Rabinovici, G.D.; Knol, D.L.; van der Flier, W.M.; van Berckel, B.N.; Scheltens, P.; Visser, P.J.; Verfaillie, S.C.; Zwan, M.D. Prevalence of amyloid PET positivity in dementia syndromes: A meta-analysis. *JAMA* **2015**, *313*, 1939–1950. [[CrossRef](#)]
71. Haller, S.; Garibotto, V.; Kövari, E.; Bouras, C.; Xekardaki, A.; Rodriguez, C.; Lazarczyk, M.J.; Giannakopoulos, P.; Lovblad, K.-O. Neuroimaging of dementia in 2013: What radiologists need to know. *Eur. Radiol.* **2013**, *23*, 3393–3404. [[CrossRef](#)]
72. Schütz, L.; Lobsien, D.; Fritzsche, D.; Tiepolt, S.; Werner, P.; Schroeter, M.L.; Berrouschot, J.; Saur, D.; Hesse, S.; Jochimsen, T. Feasibility and acceptance of simultaneous amyloid PET/MRI. *Eur. J. Nucl. Med. Mol. Imaging* **2016**, *43*, 2236–2243. [[CrossRef](#)]
73. Chiotis, K.; Carter, S.F.; Farid, K.; Savitcheva, I.; Nordberg, A. Amyloid PET in European and North American cohorts; and exploring age as a limit to clinical use of amyloid imaging. *Eur. J. Nucl. Med. Mol. Imaging* **2015**, *42*, 1492–1506. [[CrossRef](#)] [[PubMed](#)]
74. Jack, C.R., Jr.; Wiste, H.J.; Weigand, S.D.; Therneau, T.M.; Lowe, V.J.; Knopman, D.S.; Gunter, J.L.; Senjem, M.L.; Jones, D.T.; Kantarci, K. Defining imaging biomarker cut points for brain aging and Alzheimer's disease. *Alzheimer's Dement.* **2017**, *13*, 205–216. [[CrossRef](#)] [[PubMed](#)]
75. Klunk, W.E.; Koeppe, R.A.; Price, J.C.; Benzinger, T.L.; Devous, M.D., Sr.; Jagust, W.J.; Johnson, K.A.; Mathis, C.A.; Minhas, D.; Pontecorvo, M.J. The Centiloid Project: Standardizing quantitative amyloid plaque estimation by PET. *Alzheimer's Dement.* **2015**, *11*, 1–15.e14. [[CrossRef](#)] [[PubMed](#)]
76. Rowe, C.C.; Jones, G.; Doré, V.; Pejoska, S.; Margison, L.; Mulligan, R.S.; Chan, J.G.; Young, K.; Villemagne, V.L. Standardized expression of 18F-NAV4694 and 11C-PiB β -amyloid PET results with the Centiloid Scale. *J. Nucl. Med.* **2016**, *57*, 1233–1237. [[CrossRef](#)] [[PubMed](#)]
77. Rowe, C.C.; Doré, V.; Jones, G.; Baxendale, D.; Mulligan, R.S.; Bullich, S.; Stephens, A.W.; De Santi, S.; Masters, C.L.; Dinkelborg, L. 18 F-Florbetaben PET beta-amyloid binding expressed in Centiloids. *Eur. J. Nucl. Med. Mol. Imaging* **2017**, *44*, 2053–2059. [[CrossRef](#)]
78. Battle, M.R.; Pillay, L.C.; Lowe, V.J.; Knopman, D.; Kemp, B.; Rowe, C.C.; Doré, V.; Villemagne, V.L.; Buckley, C.J. Centiloid scaling for quantification of brain amyloid with [¹⁸F] flutemetamol using multiple processing methods. *EJNMMI Res.* **2018**, *8*, 107. [[CrossRef](#)]
79. Amadoru, S.; Doré, V.; McLean, C.A.; Hinton, F.; Shepherd, C.E.; Halliday, G.M.; Leyton, C.E.; Yates, P.A.; Hodges, J.R.; Masters, C.L. Comparison of amyloid PET measured in Centiloid units with neuropathological findings in Alzheimer's disease. *Alzheimer's Res. Ther.* **2020**, *12*, 22. [[CrossRef](#)]
80. Minoshima, S.; Frey, K.A.; Koeppe, R.A.; Foster, N.L.; Kuhl, D.E. A diagnostic approach in Alzheimer's disease using three-dimensional stereotactic surface projections of fluorine-18-FDG PET. *J. Nucl. Med.* **1995**, *36*, 1238–1248.
81. Minoshima, S.; Koeppe, R.A.; Frey, K.A.; Kuhl, D.E. Anatomic standardization: Linear scaling and nonlinear warping of functional brain images. *J. Nucl. Med.* **1994**, *35*, 1528–1537.
82. Kaneta, T.; Okamura, N.; Minoshima, S.; Furukawa, K.; Tashiro, M.; Furumoto, S.; Iwata, R.; Fukuda, H.; Takahashi, S.; Yanai, K. A modified method of 3D-SSP analysis for amyloid PET imaging using [¹¹C] BF-227. *Ann. Nucl. Med.* **2011**, *25*, 732–739. [[CrossRef](#)]
83. Thientunyakit, T.; Sethanandha, C.; Muangpaisan, W.; Minoshima, S. Relationship between amyloid deposition and cerebral glucose metabolism in cognitively normal elderly, patients with mild cognitive impairment and Alzheimer's dementia. *J. Nucl. Med.* **2019**, *60*, 1458.
84. Barthel, H.; Sabri, O. Clinical use and utility of amyloid imaging. *J. Nucl. Med.* **2017**, *58*, 1711–1717. [[CrossRef](#)] [[PubMed](#)]
85. Grundman, M.; Johnson, K.A.; Lu, M.; Siderowf, A.; Arora, A.K.; Skovronsky, D.M.; Mintun, M.A.; Pontecorvo, M.J. Effect of amyloid imaging on the diagnosis and management of patients with cognitive decline: Impact of appropriate use criteria. *Dement. Geriatr. Cogn. Disord.* **2016**, *41*, 80–92. [[CrossRef](#)]
86. Leuzy, A.; Chiotis, K.; Lemoine, L.; Gillberg, P.-G.; Almkvist, O.; Rodriguez-Vieitez, E.; Nordberg, A. Tau PET imaging in neurodegenerative tauopathies—Still a challenge. *Mol. Psychiatry* **2019**, *24*, 1112–1134. [[CrossRef](#)] [[PubMed](#)]
87. Buée, L.; Bussièrre, T.; Buée-Scherrer, V.; Delacourte, A.; Hof, P.R. Tau protein isoforms, phosphorylation and role in neurodegenerative disorders. *Brain Res. Brain Res. Rev.* **2000**, *33*, 95–130. [[CrossRef](#)]

88. Josephs, K.A. Current Understanding of Neurodegenerative Diseases Associated with the Protein Tau. *Mayo Clin. Proc.* **2017**, *92*, 1291–1303. [[CrossRef](#)]
89. Irwin, D.J. Tauopathies as clinicopathological entities. *Park. Relat. Disord.* **2016**, *22* (Suppl. 1), S29–S33. [[CrossRef](#)]
90. Villemagne, V.L.; Okamura, N. Tau imaging in the study of ageing, Alzheimer’s disease, and other neurodegenerative conditions. *Curr. Opin. Neurobiol.* **2016**, *36*, 43–51. [[CrossRef](#)]
91. Wang, Y.T.; Edison, P. Tau imaging in neurodegenerative diseases using positron emission tomography. *Curr. Neurol Neurosci Rep.* **2019**, *19*, 45.
92. Brendel, M.; Palleis, C.; Prix, C.; Finze, A.; Boetzel, K.; Danek, A.; Höllerhage, M.; Beyer, L.; Sauerbeck, J.; Rauchmann, B.; et al. 18F-PI-2620 tau-PET in corticobasal syndrome (ActiGliA cohort). *Alzheimer’s Dement.* **2020**, *16*, e041469. [[CrossRef](#)]
93. Brendel, M.; Barthel, H.; van Eimeren, T.; Marek, K.; Beyer, L.; Song, M.; Palleis, C.; Gehmeyr, M.; Fietzek, U.; Respondek, G.; et al. Assessment of 18F-PI-2620 as a Biomarker in Progressive Supranuclear Palsy. *JAMA Neurol.* **2020**, *77*, 1408–1419. [[CrossRef](#)]
94. Okamura, N.; Harada, R.; Ishiki, A.; Kikuchi, A.; Nakamura, T.; Kudo, Y. The development and validation of tau PET tracers: Current status and future directions. *Clin. Transl. Imaging* **2018**, *6*, 305–316. [[CrossRef](#)] [[PubMed](#)]
95. Kroth, H.; Oden, F.; Molette, J.; Schieferstein, H.; Capotosti, F.; Mueller, A.; Berndt, M.; Schmitt-Willich, H.; Darmency, V.; Gabellieri, E.; et al. Discovery and preclinical characterization of [¹⁸F]PI-2620, a next-generation tau PET tracer for the assessment of tau pathology in Alzheimer’s disease and other tauopathies. *Eur. J. Nucl. Med. Mol. Imaging* **2019**, *46*, 2178–2189. [[CrossRef](#)] [[PubMed](#)]
96. Burkett, B.J.; Johnson, D.R.; Lowe, V.J. Evaluation of Neurodegenerative Disorders with Amyloid- β , Tau, and Dopaminergic PET Imaging: Interpretation Pitfalls. *J. Nucl. Med. Off. Publ. Soc. Nucl. Med.* **2024**, *65*, 829–837. [[CrossRef](#)] [[PubMed](#)]

Disclaimer/Publisher’s Note: The statements, opinions and data contained in all publications are solely those of the individual author(s) and contributor(s) and not of MDPI and/or the editor(s). MDPI and/or the editor(s) disclaim responsibility for any injury to people or property resulting from any ideas, methods, instructions or products referred to in the content.